TWO-POINT CORRELATION ANALYSIS OF NEUTRALLY STRATIFIED FLOW WITHIN AND ABOVE A FOREST FROM LARGE-EDDY SIMULATION

HONG-BING SU[1,2]*, ROGER H. SHAW[1] and KYAW THA PAW U[1]

[1]*Atmospheric Science Program, University of California, Davis, California, U.S.A.;* [2]*Department of Geography, Indiana University, Bloomington, Indiana, U.S.A.*

Abstract. Two-point space-time correlations of velocities, a passive scalar and static pressure are calculated using the resolvable flow fields computed by large-eddy simulation (LES) of neutrally stratified flow within and above a sparse forest. Zero-time-lag spatial auto-correlation contours in the streamwise-vertical cross-section for longitudinal and lateral velocities and for a scalar are tilted from the vertical in the downstream direction, as is typical in near-wall sheared flow. On the other hand, auto-correlations of vertical velocity and of static pressure are vertically coherent. Zero-time-lag spatial auto-correlations in the spanwise-vertical cross-section show no distinct tilt, and those for both longitudinal and vertical velocities demonstrate distinct negative side lobes in the middle forest and above, while longitudinal velocity in the subcrown trunk space is laterally in-phase. Static pressure perturbations appear to be spatially coherent in the spanwise direction at all heights, especially inside the forest. Near the forest floor, longitudinal velocity is found to be in-phase with static pressure perturbation and to be closely linked to the instantaneous streamwise pressure gradient, supporting a previous proposal that longitudinal velocity in this region is dominantly modulated by the pressure patterns associated with the coherent sweep/ejection events. Near treetop height, a lack of linkage between the pressure gradient and the local time derivative of the longitudinal velocity supports the hypothesis of advection dominating turbulent flow.

The major phase characteristics of the two-point correlations essentially remained the same from four LES runs with different domain size and/or grid resolution. A larger LES domain yielded better agreement with field observations in a real forest on both the magnitudes of the correlations and the single-point integral time scales. A finer grid resolution in the LES led to a faster rate of decrease of correlation with increasing separation in space or time, as did the higher frequency fluctuations in the turbulent records from field measurements. Convective velocities estimated from the lagged two-point auto-correlations of the calculated flow fields were compared with similar calculations from wind-tunnel studies. At the canopy top, estimates from the correlation analyses agree with the translation velocity estimated from instantaneous snapshots of a scalar microfront using both LES and field data. This translation velocity is somewhat higher than the local mean wind speed. Convective velocities estimated from lagged correlations increase with height above the canopy. It is suggested that an appropriate filtering procedure may be necessary to reduce the effects of small-scale random turbulence, as was reported in a study over an orchard canopy. The mean longitudinal velocity near the treetops is found to be more appropriate than the local mean longitudinal velocity at each height to link single-point integral time scales with directly calculated spatial integral streamwise length scales.

---

* Current address: Department of Geography, Indiana University, Student Building 120, Bloomington, IN 47405, U.S.A. E-mail: hsu@indiana.edu

1. Introduction

Studies based on observations in the field (Gao et al., 1989; Bergström and Hög-ström, 1989) and in the wind tunnel (Raupach et al., 1986) have demonstrated that large organized turbulent motions dominate the transport of momentum, heat and mass within and above plant canopies. Lagged two-point correlations with vertical separations have been calculated in several previous studies to delineate the spatial characteristics of coherent structures in a streamwise-vertical plane (Raupach et al., 1989, 1991; Shaw et al., 1990; Shaw and Zhang, 1992). The two-point correlation statistics presented by Shaw et al. (1995) were based upon a wind-tunnel experiment within and above an artificial wheat canopy. Longitudinal and vertical velocities were simultaneously measured at two locations with a range of spatial separations not only in the vertical but also in the streamwise and spanwise directions. It is believed that large coherent structures strongly influence the two-point correlations, and information regarding the structures is preserved in the correlation tensor (Moin and Moser, 1989). Shaw et al. (1995) demonstrated the downwind tilt of longitudinal velocity and the vertical coherence of vertical velocity using two-point correlations. They also directly calculated the streamwise, spanwise and vertical Eulerian integral length scales, and the velocity at which large coherent structures are convected downstream. It was found that the local mean velocity is not a suitable proxy for the convective velocity (determined by correlation) in the application of Taylor's hypothesis.

Lumley's proper orthogonal decomposition (POD) (Berkooz et al., 1993) has been used to analyze coherent structures in large-eddy simulation (LES) of channel flow (Moin and Moser, 1989) and of the atmospheric boundary layer (Wilson, 1996; Wilson and Wyngaard, 1996). These researchers believed that major characteristics of large coherent structures can be revealed based upon a few principal orthogonal components extracted from the space-time correlation tensor. For example, Zhuang (1996) used POD analysis in the development of a lower-order model of coherent structures in the convective atmospheric surface layer. As a first step towards applying POD to the flow within and above a plant canopy, it is fundamental and illustrative to examine characteristics of the two-point correlation tensor. Information obtained from the two-point correlations in physical space might, in the future, be used to guide POD analysis in phase space.

A complete description of turbulent structure relies on knowledge of the velocity and pressure fields. In addition, scalar fields have often been used to identify coherent structures in field studies (Gao et al., 1989; Bergström and Högström, 1989). Shaw et al. (1990) and Shaw and Zhang (1992) demonstrated that the surface pressure pattern beneath a deciduous forest is closely related to coherent structures identified by the time trace of temperature and velocity. Zhuang and Amiro (1994) retrieved the pressure patterns during coherent motions by solving a two-dimensional Poisson equation. In all of these studies, Taylor's hypothesis was used to convert single-point time series into longitudinal distributions of velocity

and/or temperature, because it was impractical to operate a large number of velocity and scalar sensors simultaneously to measure the spatial fields in a real forest. Two main limitations in the above studies are (1) only characteristics in a streamwise-vertical plane can be revealed; and (2) Taylor's hypothesis may be incorrectly applied, if one chooses an inappropriate convective velocity, as discussed by Shaw et al. (1995).

Large-eddy simulation is a computational scheme that directly resolves those scales of motion equal to or larger than twice the grid mesh (mesh size 1 m to 2 m in this study) and parameterizes the subgrid-scale (SGS) variances and covariances. As a source of well-controlled, three-dimensional and time dependent flow fields within and above a plant canopy, LES provides greater detail of the velocity, static pressure, and passive scalar fields that complement observations in the wind tunnel and the field. Especially, such detailed information is much needed for the study of the spatial characteristics of large organized turbulent structures, within and above tall canopies, such as a forest. Statistical properties derived from two-point space-time correlations, such as the integral time and length scales are very useful and are often used in Lagrangian modelling studies to distinguish diffusion in the near field and far-field within and above plant canopies (Raupach, 1989).

This study investigates the statistical properties of the sweep/eject cycle and its influence on flow statistics within and above a forest using two-point correlation analysis of the resolved-scale flow field computed by large-eddy simulation. Eulerian integral length scales in both streamwise and spanwise directions are directly calculated from the two-point spatial correlations without the assumption of Taylor's hypothesis. Single-point integral time scales are also calculated and compared with field observations. In addition, convective velocities are estimated from lagged correlations and compared with those obtained in previous wind-tunnel and field observations. Four LES runs have been performed to investigate the effects of the domain size and grid resolution on the two-point correlation statistics. These are discussed along with the effects of record length and temporal resolution in field observations.

2. Methodology

2.1. DEFINITION OF TWO-POINT CORRELATION

The two-point space-time correlation coefficient tensor R_{ij} between vector or scalar variables, X_i and X_j, is defined in the following expression:

$$R_{ij}(r_x, r_y, z, z', \tau) = \frac{\overline{X_i(x, y, z, t) X_j(x + r_x, y + r_y, z', t + \tau)}}{[\overline{X_i(x, y, z, t)^2} \, \overline{X_j(x + r_x, y + r_y, z', t + \tau)^2}]^{1/2}}, \quad (1)$$

where each variable is a departure from its mean, and indices i and j refer to the elements of a state vector that includes velocity, scalar concentration, static

pressure, and temporal rates of change or spatial gradients of such quantities; an overbar represents a time and space average as detailed in Section 2.3; x, y and z define streamwise or longitudinal, spanwise or lateral, and vertical locations of the variable X_i, at time t; whereas the variable X_j is located at $x + r_x$, $y + r_y$ and z', at time $t + \tau$; r_x and r_y are horizontal separations from X_i to X_j in the streamwise and spanwise directions, respectively; τ is a time lag imposed on the variable X_j. The quantity R_{ij} is considered an auto-correlation when $X_i = X_j$ (X_i and X_j being the same physical variable) or a cross-correlation when $X_i \neq X_j$, regardless of whether the separation is in time or space. For stationary, horizontally homogeneous turbulence, one may expect certain symmetry relationships, e.g., $R_{ij}(r_x, r_y, z, z', \tau) = R_{ij}(r_x, -r_y, z, z', \tau)$, but no deliberate attempt was made to force any such relationship on the correlation fields computed from our simulations and presented here.

2.2. Definitions of Eulerian integral time and length scales

2.2.1. *Single-point Integral Time Scale*
When the two variables X_i and X_j are spatially collocated ($r_x = 0$, $r_y = 0$ and $z = z'$) and a time lag is imposed on X_j, Equation (1) represents a single-point lagged correlation. An Eulerian integral time scale $T(X_i, X_j, z)$ is defined as:

$$T(X_i, X_j, z) = \frac{1}{R_{ij}(0, 0, z, z, 0)} \int_0^\infty R_{ij}(0, 0, z, z, \tau)\mathrm{d}\tau, \tag{2}$$

where the normalizing factor $R_{ij}(0, 0, z, z, 0)$ accommodates cases when $X_i \neq X_j$, and $-1 < R_{ij}(0, 0, z, z, 0) < 1$. Usually, the upper limit of the integral in Equation (2) is reduced from infinity to the time lag when the first zero-crossing occurs.

2.2.2. *Spatial Integral Length Scales*
Eulerian spatial integral length scales in the streamwise direction $L_x(X_i, X_j, z)$ and the spanwise direction $L_y(X_i, X_j, z)$ are defined as:

$$L_x(X_i, X_j, z) = \frac{1}{R_{ij}(0, 0, z, z, 0)} \int_0^\infty R_{ij}(r_x, 0, z, z, 0)\mathrm{d}r_x, \tag{3}$$

$$L_y(X_i, X_j, z) = \frac{1}{R_{ij}(0, 0, z, z, 0)} \int_0^\infty R_{ij}(0, r_y, z, z, 0)\mathrm{d}r_y, \tag{4}$$

where the normalizing factor $R_{ij}(0, 0, z, z, 0)$ accommodates cases when $X_i \neq X_j$, and $-1 < R_{ij}(0, 0, z, z, 0) < 1$. The two variables X_i and X_j are located at the same height ($z = z'$), and there is no time lag imposed on X_j ($\tau = 0$). In practice, the upper limit of the integral is reduced from infinity to the horizontal separation where the first zero-crossing is located, if it occurs prior to the greatest separation

Basic information about the four LES runs. The time interval and time period are for the time series of the x-z and y-z slices in the LES outputs.

LES Run	A	B	C	D
$N_x \times N_y \times N_z$	$96 \times 96 \times 30$	$96 \times 96 \times 60$	$192 \times 192 \times 60$	$192 \times 192 \times 60$
Grid spacing (m)	2	2	1	2
Time interval (s)	1	1	0.4	1
Time period (min)	20	30	15	20
U_{hc} (m s^{-1})	0.95	0.97	0.95	0.99
u_* (m s^{-1})	0.27	0.28	0.27	0.30

allowed by the horizontal domain. Shaw et al. (1995) discussed modifications to this definition in certain situations.

2.3. LES ANALYSIS

Details of the large-eddy simulation, including subgrid-scale parameterization, major driving forcing, upper boundary condition, and the model forest are described in detail by Su et al. (1998a). For the present analysis, three more LES runs were carried out in addition to the run presented in Su et al. (1998a), which is denoted here as run A, to investigate the effects of domain size and grid resolution. The numbers of equally-spaced grids in the streamwise (N_x), spanwise (N_y) and vertical directions (N_z), and the grid spacing for each LES run are given in Table 1, along with the values of mean longitudinal velocity at treetop level (U_{hc}) and friction velocity (u_*). The model forest remains the same for all LES runs, with a forest height (h_C) of 20 m and a leaf area index (LAI) of 2. The vertical profile of the leaf area density was given in Su et al. (1998a). The vertical domain extends to six times the canopy height, and the largest horizontal extent of the LES domain is more than 19 times the canopy height. Boundary conditions are periodic in the horizontal directions; thermal stratification is set to neutral.

The LES output used in this study include time series of an x-z slice and of a y-z slice saved at a constant time interval over a specified time period (Table I) after the flow had reached an equilibrium state. The time series of the x-z slices were used to calculate zero-time-lag two-point correlations with vertical and streamwise separations, and lagged two-point correlations with only streamwise separations. Time series of y-z slices were used to calculate zero-time-lag two-point correlations with vertical and spanwise separations. The y-z slices were also used to calculate lagged two-point correlations with vertical separations only, which become lagged single-point correlations when $z' = z$.

Since the boundary conditions are periodic in the horizontal, the correlation fields were further averaged over all locations in the x-direction or in the y-direction, and horizontal separations r_x and r_y are defined in the range from $-9.6h_C$ to $9.5h_C$. However, in the vertical direction, correlations are presented only up to three times the canopy height ($z'/h_C = 3$). This is because, (1) correlations within and immediately above the forest are our main interest; (2) observations in a real forest used in this study were only available up to 2.5 times canopy height; and (3) we have decreased confidence in the correlations at higher levels due to the limited LES vertical domain. In the horizontal directions, organized patterns of the space-time correlations associated with the coherent motions are often less than the range of $-9.6h_C$ to $9.5h_C$. Thus, to amplify these correlation patterns, we do not always present the correlations from run D to the greatest horizontal separation available.

2.4. FIELD DATA ANALYSIS

Turbulent velocity and temperature were collected at 10 Hz from ultrasonic anemometer-thermometers (Kaijo Denki Co. Ltd.) positioned at seven locations on two scaffolding-type towers within and above a deciduous forest near the northern perimeter of the Camp Borden military base in Ontario, Canada during September and October, 1986. The average height of the forest was about 18 m, which is close to the height of the model forest in our LES. The leaf area index was 2.6 on calendar day 274, and 2.1 on day 281 (Neumann et al., 1989), and leaf area density profiles were close to that used in the LES (Su et al., 1998a). More detailed descriptions of the site and experiment can be found in Shaw et al. (1988). Nine 30-minute periods of data were selected for the comparison of single-point statistics with the LES in Su et al. (1998a), which were also used in the present two-point correlation analysis. The criteria for the data selection were: (1) near-neutral stratification; (2) mean wind from a direction of sufficient upwind fetch; (3) leaf area index and leaf area density profile close to the model forest in the LES; and (4) sensors at all seven locations functioning properly. The data used in this study include five 30-minute periods of three-dimensional velocities during calendar days 280 and 281 under near neutral conditions, and four 30-minute periods of temperature fluctuations on day 275 under unstable conditions. A coordinate rotation was performed to force the local mean lateral and vertical velocities of each 30-minute period to zero.

To investigate the effects of record length and temporal resolution of the field observations on the lagged correlations with vertical separations and on the single-point integral time scales, each 30-minute 10 Hz time series was also divided into 5-minute segments, and/or filtered by a moving average with a time window of three seconds.

3. Results and Discussion

3.1. CORRELATIONS IN THE x-z PLANE

Both the wind-tunnel study of Shaw et al. (1995) and our current simulations yield zero-time-lag correlations with spatial separations in both the streamwise and vertical directions. Observations in real forests (Shaw et al., 1990; Raupach et al., 1991; Shaw and Zhang, 1992) had only simultaneous measurements of turbulent velocity and temperature available at a few points from a single tower. To match temporal correlations computed from such field data with LES and wind-tunnel simulations with streamwise separations, we normalized the time lag as $-\tau U_{hc}/h_C$. Spatial separations were also normalized with the canopy height h_C.

3.1.1. *Auto-Correlations*

The positive contours (with a maximum of 1 at $r_x/h_C = 0$ and $z'/h_C = 1$) of zero-time-lag auto-correlations of longitudinal velocity (u), lateral velocity (v) and the scalar (s) (Figures 1–3) have elongated shapes, and exhibit a downwind tilt from the vertical. Peak correlations at an increasing vertical separation above or below the treetops (reference) occur at a larger longitudinal distance downstream or upstream from the reference. Auto-correlations of vertical velocity do not show any such tilt (Figure 4). These phase characteristics are typical of near-wall sheared flows, and are in general agreement with previous wind-tunnel (Shaw et al., 1995) and field (Raupach et al., 1991; Shaw and Zhang, 1992) observations within and above plant canopies. In addition, our LES shows that static pressure perturbations (p') are also vertically coherent (Figure 5), and the auto-correlation of p' remains greater than 0.7 within the forest. Since pressure is calculated as a spatial integration of the velocity field, the strongly in-phase nature of static pressure perturbations at different levels suggests that they are mostly determined by air motions in a single region. This region is most likely to be the upper forest and layers immediately above the forest, where vertical shear of the longitudinal velocity is strongest. Shaw et al. (1990) demonstrated that the velocity field in this region contributed the most to wall pressure perturbations. Field observation (Conklin and Knoerr, 1994) and our LES (Su, 1996) showed that the most significant static pressure perturbations are mainly associated with coherent motions (defined by sweep/ejection and scalar microfront) and vertically in-phase inside forest canopies. The pressure patterns that Zhuang and Amiro (1994) presented from solutions of a two-dimensional Poisson equation using time series of turbulent velocity and temperature within and above the Camp Borden forest were also vertically coherent.

  The downwind tilt in the auto-correlations of u', v' and s' may be quantified by a slope angle α (from the horizontal plane). We estimated α from two different definitions using correlation contours greater than or equal to 0.3. First, we performed a linear regression over all the points of ($r_{x,\max}, z' - z$), where $r_{x,\max}$ is the horizontal separation that maximizes the correlation for a given vertical separation $z' - z$. In
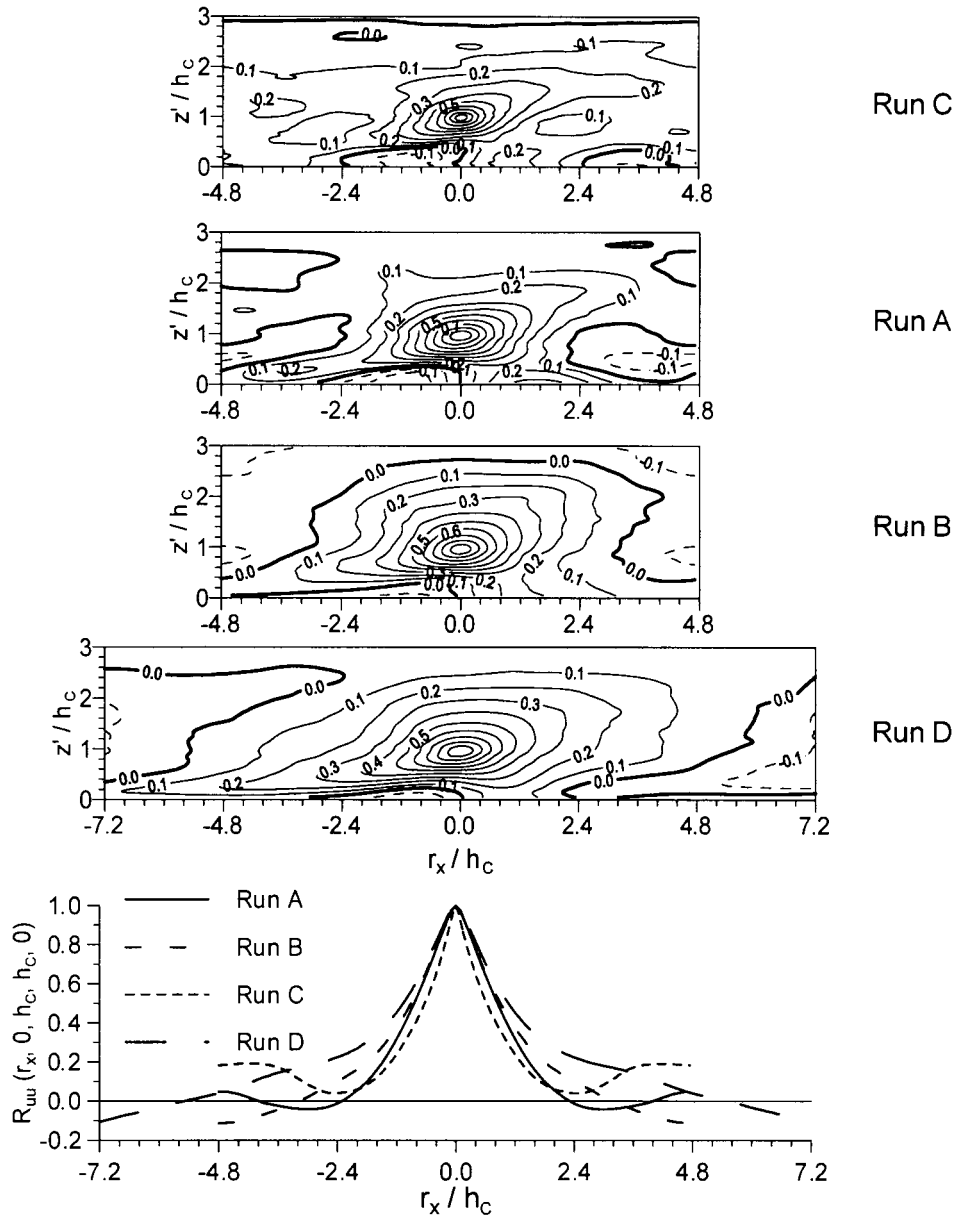
Figure 1. Zero-time-lag two-point auto-correlation with streamwise and vertical separations of longitudinal velocity with $r_y = 0$ and X_i at the treetops.
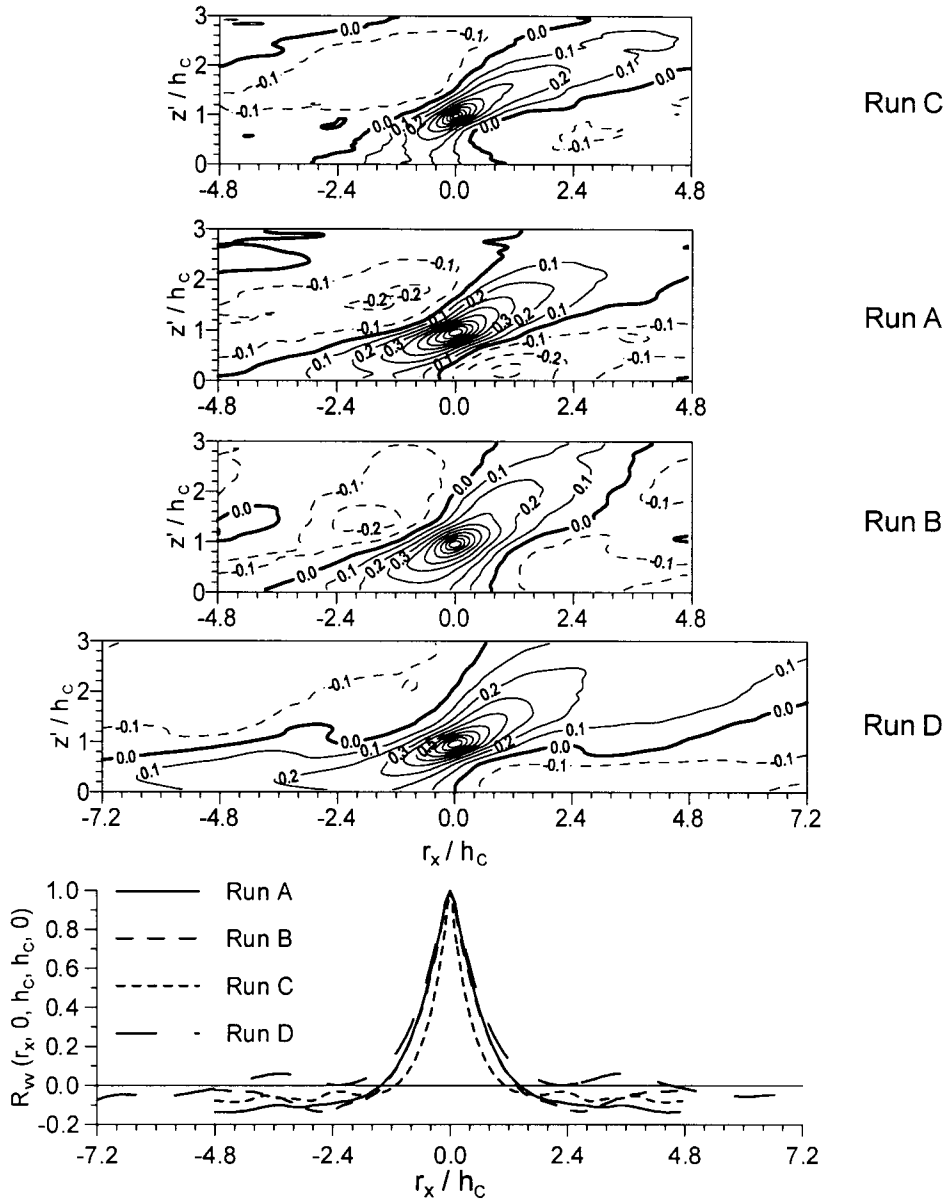
Figure 2. Same as Figure 1 but for the lateral velocity.
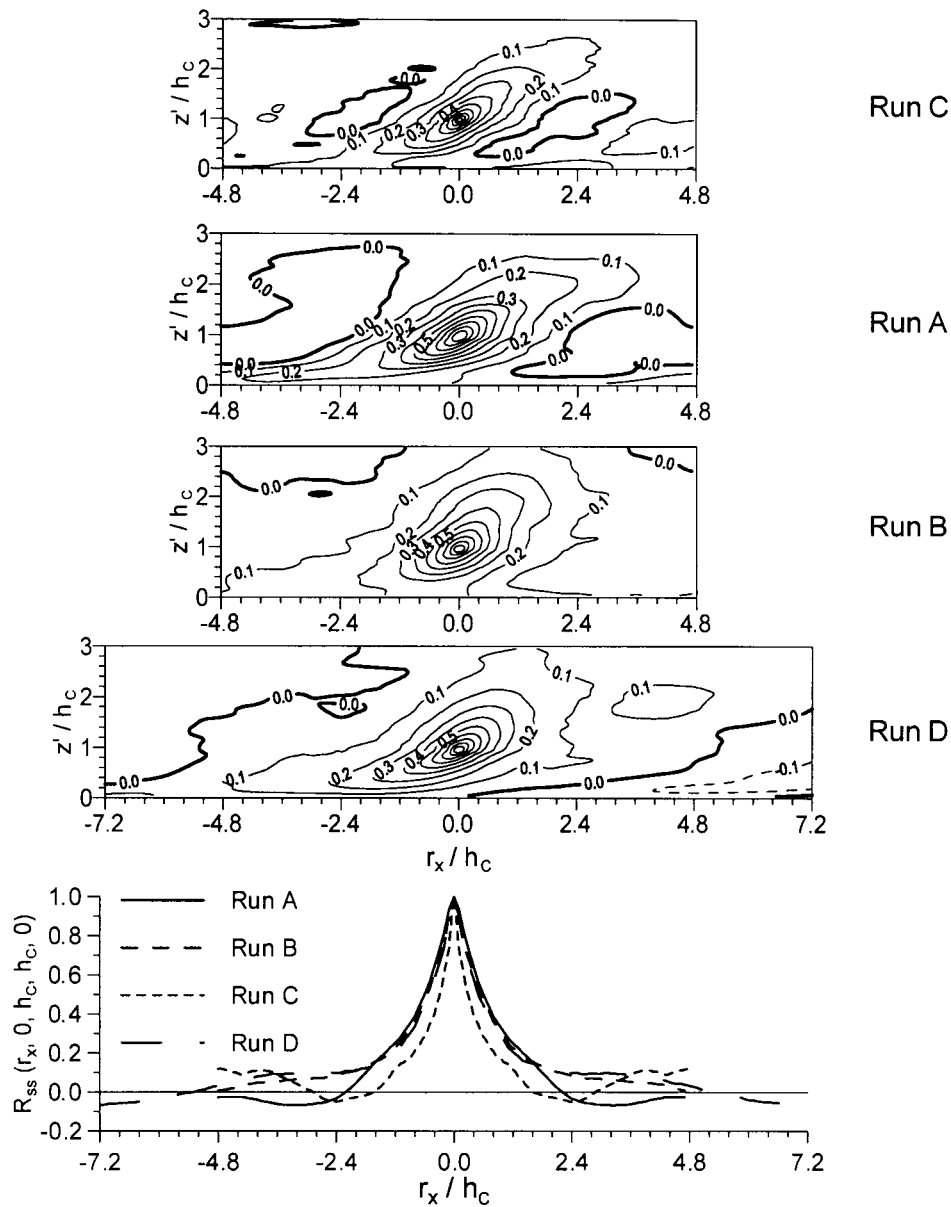
Figure 3. Same as Figure 1 but for the scalar.

the second method, the linear regression was based on all the points $(r_x, z'_{max} - z)$, where $z'_{max} - z$ is the vertical separation that maximizes the correlation for a given horizontal separation r_x. The results are summarized in Table II. Necessarily, the first method yields a greater value than the second method, and finer grid resolution (Run C) results in smaller variations of α values than coarser resolutions (Runs A,
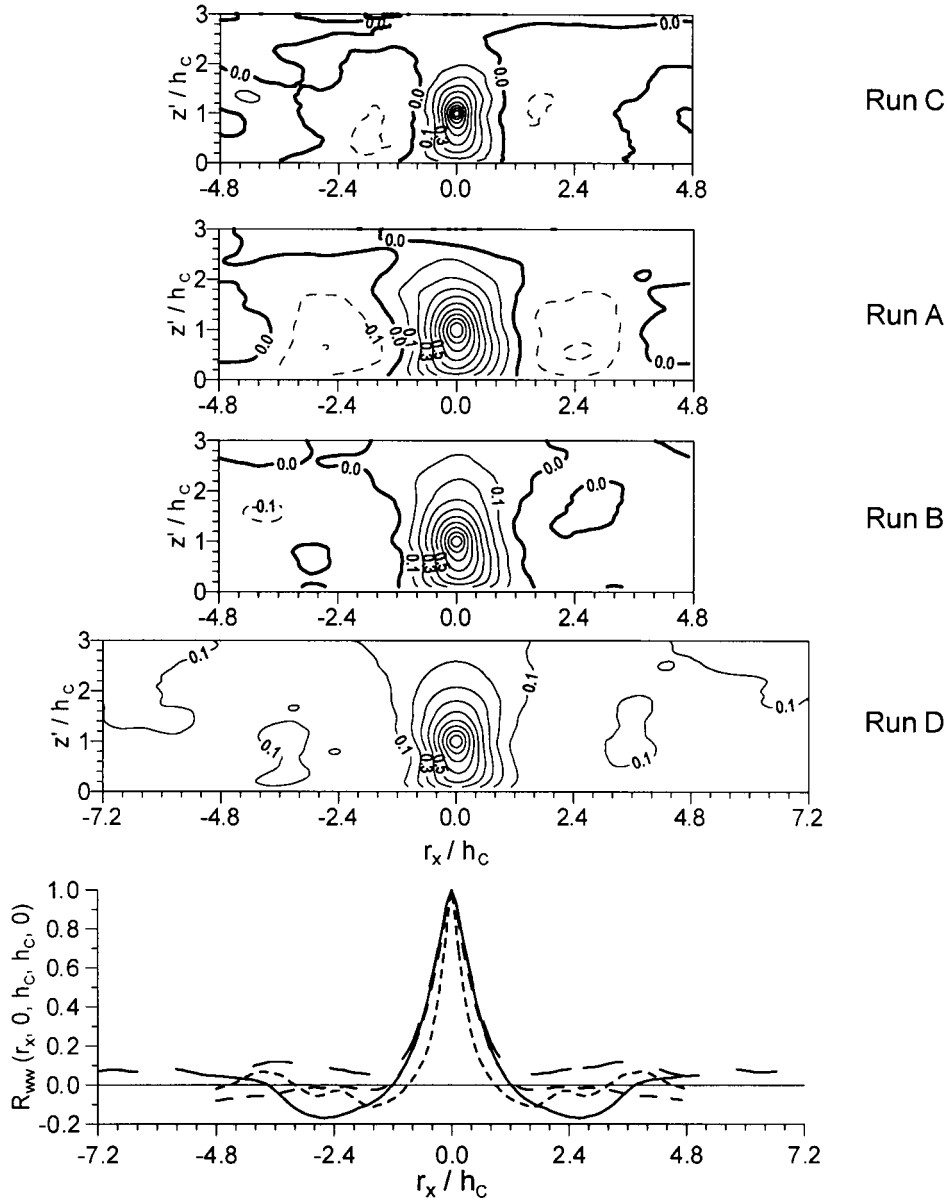
Figure 4. Same as Figure 1 but for vertical velocity.
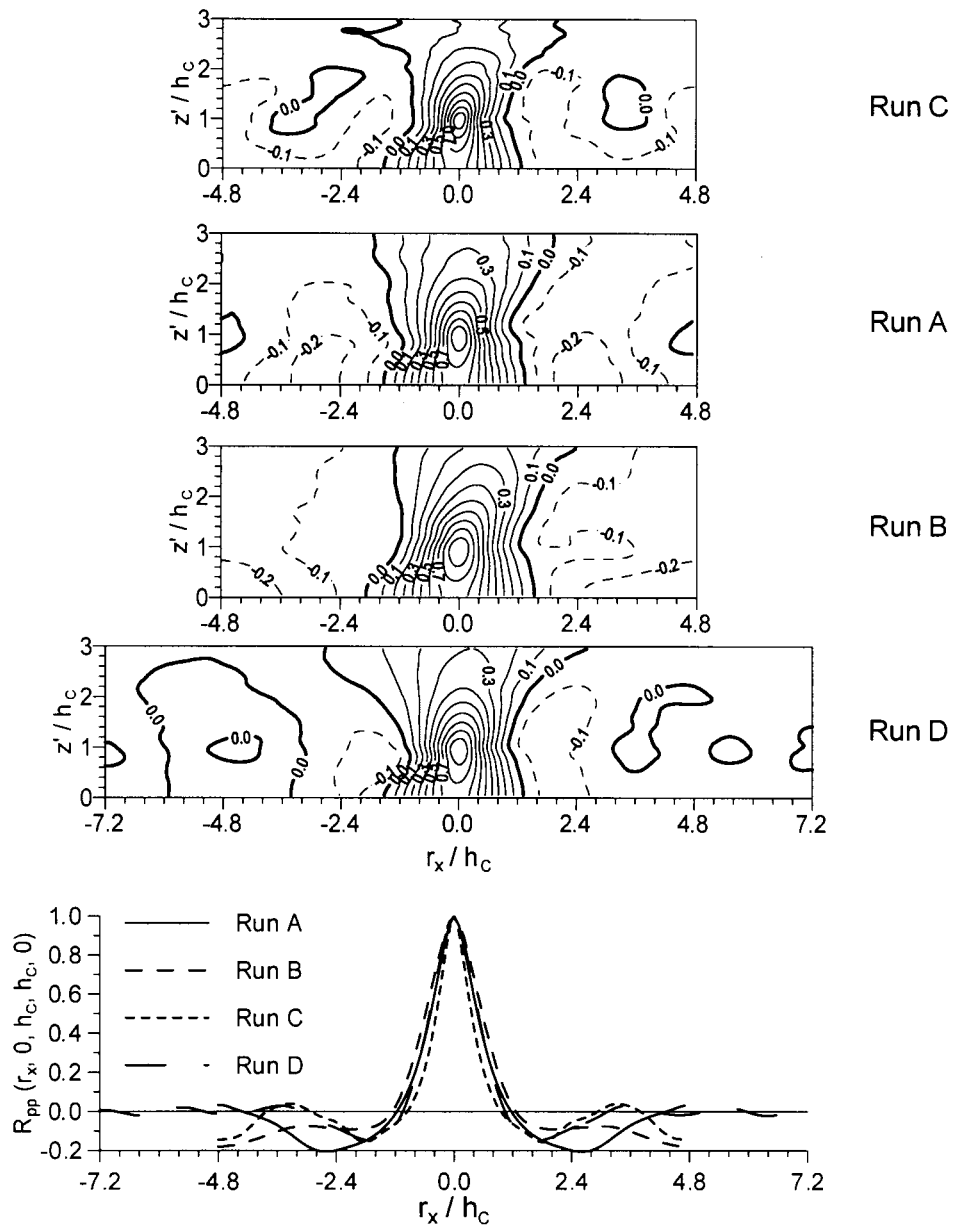
Figure 5. Same as Figure 1 but for static pressure.

TABLE II

Slope angle α (from the horizontal) calculated from zero-time-lag auto-correlations shown in Figures 1–3. Rows 2, 3 and 4 are based upon the points $(r_{x,\max}, z' - z)$, and the bottom three rows from the points $(r_x, z'_{\max} - z)$.

LES Run	A	B	C	D
$\alpha(R_{uu})$	48° ($R^2 = 0.92$)	52° ($R^2 = 0.82$)	34° ($R^2 = 0.93$)	49° ($R^2 = 0.78$)
$\alpha(R_{vv})$	34° ($R^2 = 0.99$)	43° ($R^2 = 0.99$)	36° ($R^2 = 0.98$)	33° ($R^2 = 0.98$)
$\alpha(R_{ss})$	38° ($R^2 = 0.97$)	52° ($R^2 = 0.99$)	42° ($R^2 = 0.99$)	44° ($R^2 = 0.95$)
$\alpha(R_{uu})$	13° ($R^2 = 0.95$)	10° ($R^2 = 0.94$)	16° ($R^2 = 0.95$)	11° ($R^2 = 0.97$)
$\alpha(R_{vv})$	20° ($R^2 = 0.97$)	21° ($R^2 = 0.97$)	26° ($R^2 = 0.98$)	21° ($R^2 = 0.97$)
$\alpha(R_{ss})$	23° ($R^2 = 0.98$)	26° ($R^2 = 0.85$)	28° ($R^2 = 0.97$)	20° ($R^2 = 0.98$)

B and D). Wind-tunnel measurements inside and above an artificial wheat canopy (Raupach et al., 1989, 1991; Shaw et al., 1995) provided manual estimates of the slope angle of about 18° for the major axis of the ellipse of the longitudinal velocity auto-correlations. This value agrees with the slope angle (18°) of the peak space-time velocity-wall shear stress cross-correlations measured in a turbulent boundary layer both above a smooth wall (Brown and Thomas, 1977) and the 20° angle above a rough wall (Bessem and Stevens, 1984), and is close to the α values we calculated using the second method. Not presented here for the sake of brevity is that the slope angle becomes smaller when the ground is approached, particularly in the lower half to third of the forest. This may be seen from the positive contours (with a maximum of 1 at $r_x/h_C = 0$ and $z'/h_C = 1$) in Figures 1–3 for contour levels between 0.3 and 0.1.

A unique feature of the u' auto-correlation, not present in the auto-correlations of v' and s', is that, in the trunk space (lower third of the forest), a second region of significant positive correlation (between 0.2 and 0.3) occurs downstream ($0 < r_x/h_C < 2.4$) or in advance of the reference u' at the treetops, while a region of negative correlations (between -0.1 and -0.2) follows, which is upstream ($-2.4 < r_x/h_C < 0$) of, or lags, the reference u' at treetop height. We will argue later (Section 3.1.2) that this feature is a result of u' in the two regions being modulated by a pressure pattern that is closely associated with the coherent motions. A positive correlation region ($r_x/h_C < -2.4$) near the forest floor is a continuous downward extension of the tilted positive correlation contours upstream of u' at the treetops. This can be attributed to turbulent transport, as a fast moving (gust) and low scalar concentration air parcel moves downwind and penetrates the forest, an acceleration in longitudinal velocity and a decrease in scalar concentration in the trunk space appear upstream of those near the top of the forest.

The unique pair of positive and negative correlation regions in the auto-correlation of u' discussed above was not revealed by the wind-tunnel study of

Shaw et al. (1995). This could be due to the significant difference in canopy structure (20-m tall forest versus sparse artificial wheat constructed of flexible 'stalks' of fishing line) and/or the lowest location of the triple-hot-wire probe being insufficiently close to the wind-tunnel floor.

Shaw and Zhang (1992) did present lagged auto-correlations of u' with the reference at treetop level using data collected from the Camp Borden forest, in which the lowest sonic anemometer was at about one-third of the canopy height. Their emphasis, however, was on the positive correlation at this height appearing at the downstream position, and the close correlation with pressure perturbation measured at the ground surface. Here we compare such lagged u' auto-correlations using data from the same experiment used by Shaw and Zhang (1992) with those from our LES runs A and D (Figure 6). For $z'/h_C = 0.33$ (experiment) or 0.35 (LES), positive correlation regions appear both in advance of and behind the u-signal near the canopy top in both field observations and the LES, with similar values of peak correlation (between 0.15 and 0.3). The agreements in the phase characteristics, in the normalized time lags at which peak correlations are located for a given vertical separation (Figure 7), and in the magnitudes of the peak correlations are remarkable. The same conclusions can also be made with regard to comparisons of the lagged auto-correlations of other variables (v', w' and s'), with vertical separations, between the LES output and the field observations. For the sake of brevity, only normalized time lags for peak scalar correlations are shown in Figure 7.

The main effects of domain size and grid resolution and the effects of the record length and sampling frequency of the time series of field observations on the auto-correlations shown in Figures 1–7 can be summarized as follows. First, the general phase relationships essentially remain the same for each set of auto-correlations. The downwind tilt in the auto-correlations of u', v' and s', the vertical coherence of w' and p', and the unique positive and negative correlation regions in the trunk space for u', are a few examples. Second, both domain size and grid resolution in the LES, or the record length and sampling frequency of the time series of turbulence data in the field, mainly influence the rate of decrease of auto-correlation with increasing separation in space or time.

The LES runs A, B and D have the same grid spacing, and thus allow us to exclude the effects of grid resolution when we are discussing the influence of domain size. There is little change in the auto-correlations of u' and w' inside the forest with vertical separation and the reference at the treetops (Figure 8), and all three runs (A, B and D) agree with field observations very well. However, a more extensive vertical domain (run B versus run A) did reduce the impact of the rigid upper boundary and slow down the decrease of auto-correlation with increasing vertical separation above the forest, making our LES results closer to field observations (zero-time-lag auto-correlations for the same vertical separations). The larger horizontal domain (run D) agrees with observations better than a smaller horizontal domain (run B) for the auto-correlations of w'. However, for the auto-correlations
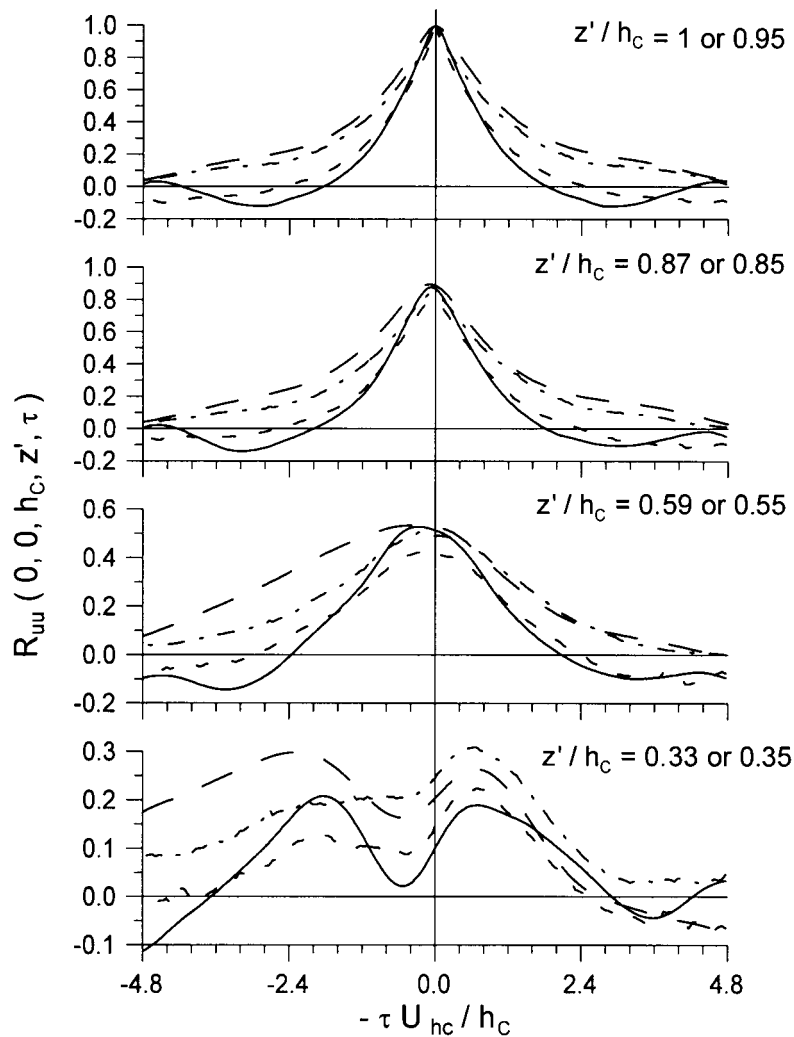
Figure 6. Lagged two-point auto-correlation of longitudinal velocity with vertical separation only ($r_x = r_y = 0$). The reference is at $z/h_C = 1$ in field observation and at $z/h_C = 0.95$ in the LES. Solid curve: LES run A; Long dashed curve: LES run D; Short dashed curve: Camp Borden data (5-minute time series at 10 Hz sampling frequency); Dash-Dot curve: Camp Borden data (30-minute length and 10 Hz frequency).

of u', at $2h_C$ and above, correlation values from the LES are still smaller than the observations by 0.1 to 0.2 (Figure 8). This is likely because the largest vertical domain in our LES is still only six times canopy height, and the ratio between the canopy height and the boundary-layer depth is much greater in our LES than would be expected in the natural atmospheric boundary layer. Thus, our simulation does not reproduce as much large-scale inactive motion (which is largely horizontal)
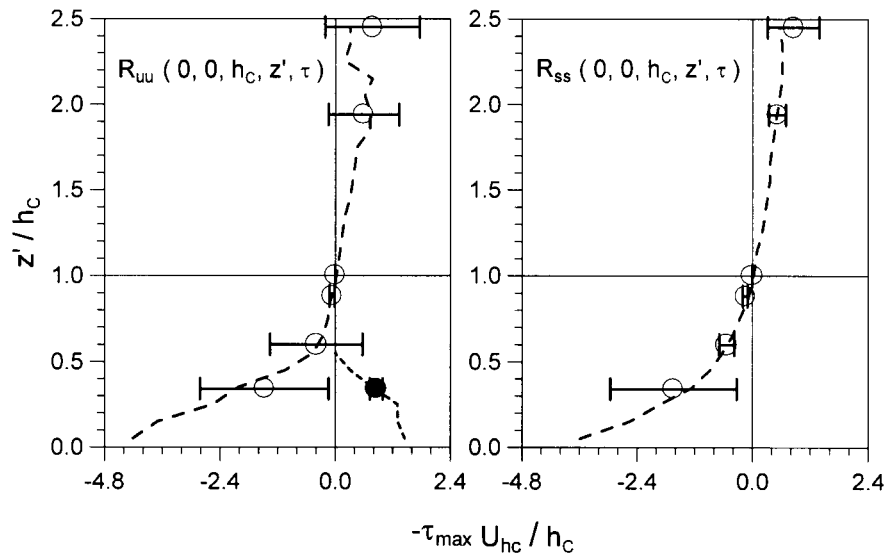
Figure 7. Normalized time lags of peak lagged two-point auto-correlations of longitudinal velocity (left) and the scalar (right) with vertical separations only ($r_x = r_y = 0$) and X_i at the treetops. Dashed curves: LES run A; Circles: Camp Borden data (5-minute time series at 0.33 Hz frequency). Note that peak auto-correlation of u' occurs both downstream and upstream of the reference at the treetops in the lower half of the forest.

as would occur naturally (Raupach et al., 1986, 1996). Evidence supporting this speculation is that a shorter record length of observations did reduce the auto-correlations of u' by more than 0.1 but reduced little the auto-correlations of w' (Figure 8). The difference in the auto-correlations of u' at higher levels between our LES and observation is not considered a serious problem in regard to the objectives of the current work, since the coherent eddies we are interested in are three dimensional, are associated with shear instability, and scale with the shear and canopy height (Raupach et al., 1996). For example, field observations of scalar microfronts from an array of towers (Zhang et al., 1992) showed that the horizontal scales of the coherent motions are on the order of 9 to 12 times canopy height in the longitudinal direction and 3 to 4 times canopy height in the lateral direction. The largest horizontal domain size in our LES runs is more than 19 times canopy height, and we considered it to be adequate for the objectives of the present work.

In addition, the impact of a larger horizontal domain on auto-correlations with streamwise separation is only significant for u' (lowest panels in Figures 1–5). The lagged auto-correlation of u' from longer time series also decreases more slowly with increasing time lag than shorter records (Figure 6). In the top panel of Figure 6, it is shown that R_{uu} from LES run D (larger domain) matches that from field data of the longer time series (30 minutes), while LES run A (smaller domain) yields a result closer to the shorter time record (5 minutes). As expected, the auto-
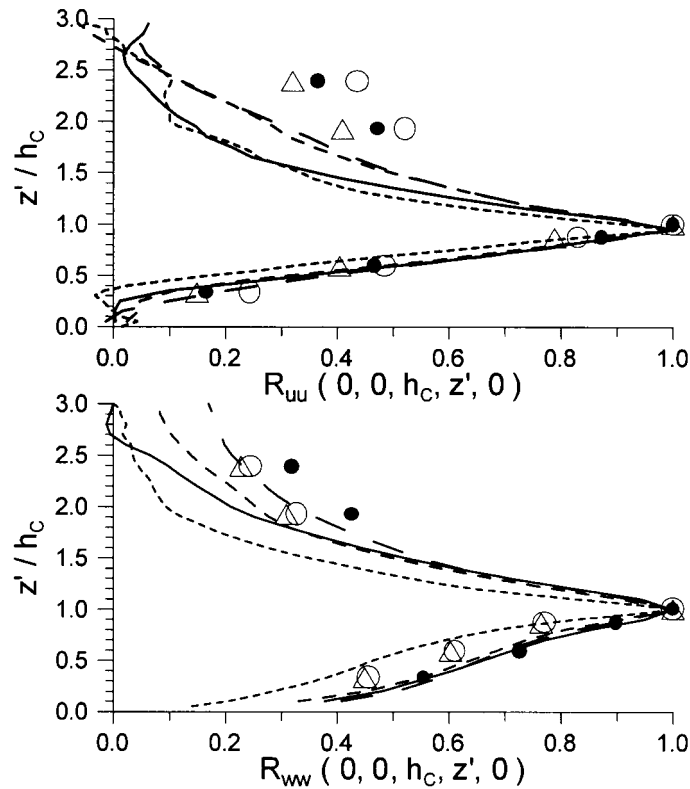
Figure 8. Two-point auto-correlations of longitudinal velocity (upper panel) and vertical velocity (lower panel) with vertical separations only ($r_x = r_y = \tau = 0$) and X_i at the treetops. Curves are from the LES (Run A: solid curve; Run B: medium dashed curve; Run C: short dashed curve; Run D: long dashed curve). Points are from Camp Borden data (Open circles: 30-minute time series and 10 Hz frequency; Open triangles: 5-minute time series at 10 Hz; Closed circles: 5-minute time series at 0.33 Hz).

correlation of p' changed little from the three runs A, B and D since it is a spatial integral of the velocity field.

Finally, both a finer grid resolution in the LES and a higher temporal response in field observations result in a faster rate of decrease of correlation with spatial separation or time lag. This is because smaller scale turbulence is more random and degrades the coherence associated with larger organized motions.

The same conclusion can be made with regard to the effects of LES domain size and grid resolution on other two-point space-time correlations. These are: (1) a particular phase characteristic essentially remains unchanged among all LES runs; (2) a more extensive domain size led to a slower rate of decrease of correlations at large spatial separations, but such effects are minimal within the forest; and (3) a finer grid resolution yielded more small-scale turbulence being resolved by the LES, which degrades the spatial coherence associated with large-scale coherent

motions. Thus, to keep our following discussion brief, we will mainly show results
from run D.

3.1.2. *Cross-Correlations*

The peak cross-correlation between u' and w' at treetop height is about -0.6
(panels 1 and 3 in Figure 9). This value agrees with the observation of Shaw et
al. (1988) from the Camp Borden forest, but is higher than a calculation made in
a wind-tunnel experiment (-0.45) by Brunet et al. (1994). Both are greater than
values observed in the atmosphere over relatively smooth surfaces (-0.3 to -0.35)
and indicate stronger mixing by the coherent motions near the top of a plant canopy.
With either u' or w' as the reference at the treetops, the negative correlations extend
to more than $2h_C$ both upstream and downwind. This may be expected if we believe
that the sweep/ejection events dominate turbulent motions near the treetops, and u'
and w' are negatively correlated in both the sweep and the ejection.

Near the forest floor, u' and w' are poorly correlated locally (-0.1), but greater
correlations occur when there is a spatial separation between them (panels 2 and
4 in Figure 9). For example, u' near the ground (panel 2 in Figure 9) is negatively
correlated with w' upwind at all heights over a streamwise distance of about $2.4h_C$,
and is positively correlated with w' downwind at all heights over a similar stream-
wise distance. The strongest negative correlation (< -0.4) is located at $z'/h_C = 0.3$
and $r_x/h_C = -0.8$, and the maximum positive correlation (> 0.3) is located near
the middle canopy and $r_x/h_C = 1$.

When u' is the reference (panels 1 and 2 in Figure 9), there is no distinct tilt in
the correlation R_{uw} contours because of the vertically in-phase nature of the vertical
velocities (Figure 4). When w' is the reference (panels 3 and 4 in Figure 9), R_{wu}
contours reflect the major characteristics of the auto-correlations of u' (Figure 1),
including the downwind tilt and two regions of positive and negative correlation,
but R_{wu} has the opposite sign from R_{uu} in the same region.

An interpretation of the cross-correlations in Figure 9 can be made on the basis
of current understanding of sweep/ejection structures and of the pressure perturb-
ations appearing in the trunk space. Streamwise velocity near the canopy top is
strongly and broadly related to vertical motion extending in the longitudinal dir-
ection distances equivalent to several canopy heights (panel 1). This is compatible
with the strong negative correlations between streamwise and vertical velocities
seen in ejection and sweep regions. Correlations between streamwise velocity near
the forest floor and vertical velocity (panel 2) are remarkably different, however.
Streamwise velocity near the forest floor is not immediately correlated with vertical
velocity but is correlated with vertical velocity with upwind (negative correlation)
and downwind (positive correlation) displacements. This is the expected result of
continuity and of the relationship between near-surface horizontal convergence or
divergence and vertical velocity. It can also be interpreted in terms of flow dy-
namics and the positive pressure perturbation expected in the zone of horizontal
convergence between an ejection and following sweep.
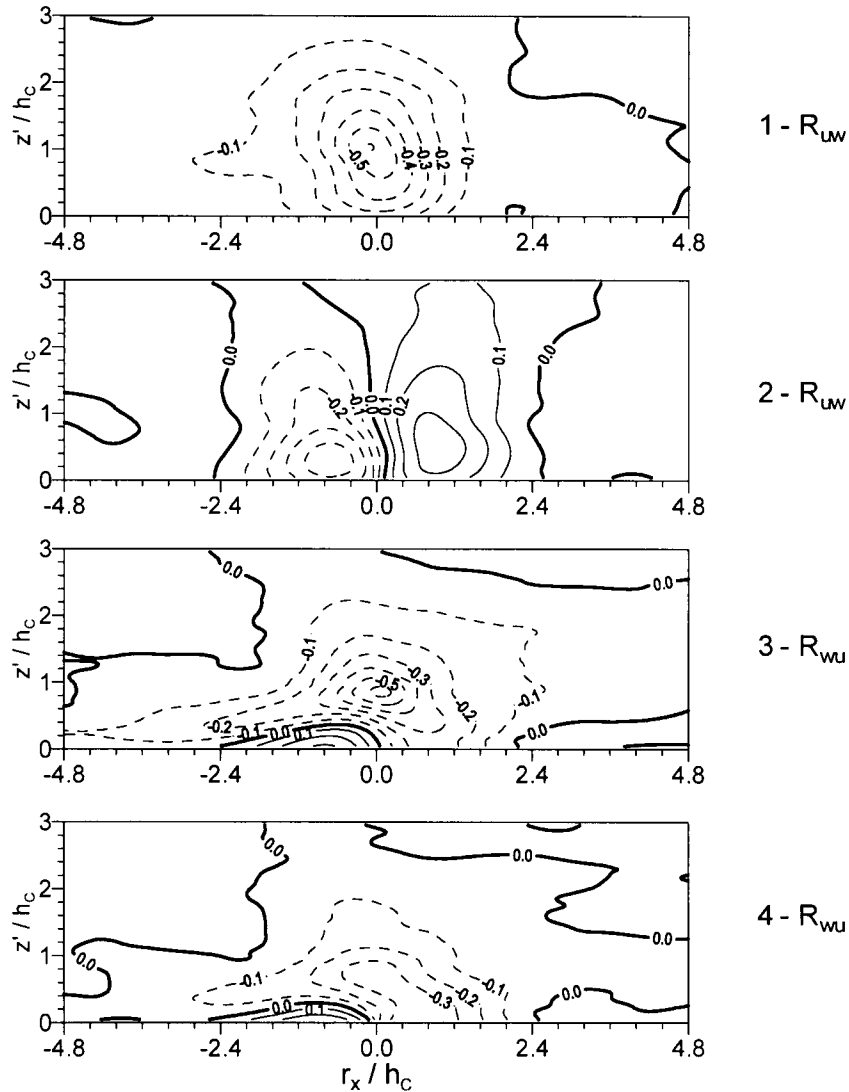
Figure 9. Zero-time-lag two-point cross-correlation between u' and w' with streamwise and vertical separations ($r_y = 0$) from LES run D. Panels 1 and 2 with $X_i = u'$; Panel 3 and 4 with $X_i = w'$; Panels 1 and 3 with X_i at $z = 0.95 h_C$; Panel 2 and 4 with X_i at $z = 0.05 h_C$.

Panel 3 of Figure 9, in which vertical velocity near the canopy top is the reference, reflects the zone of negative correlation with streamwise velocity but to a less broad extent. Indeed, the w-signal is largely uncorrelated with streamwise velocity near the surface unless a horizontal displacement is imposed on the latter. Such correlations then match those expected from the considerations given in the previous paragraph. In the last panel, with vertical velocity near the forest floor as

the reference, a similar picture appears because of the general vertical coherence of vertical velocity. Correlations are degraded, however, from those in panel 3.

Shaw and Zhang (1992) reported that longitudinal velocity deep within the canopy is strongly and positively correlated with static pressure measured at the forest floor. Peak correlation in the trunk space (about a third of canopy height) was between 0.6 and 0.7, and decreased to about 0.3 in the upper forest. Peak correlations also appeared at a larger time lag with increasing vertical distance from the ground. Our LES results (positive correlations in panel 1 in Figure 10) agree with their observation very well on both correlation magnitudes and the phase relationship. Absent in their study but present in our LES are negative correlation regions in the trunk space upwind of the positive correlations. This may be due to the fact that their lowest sonic anemometer was about one third of the canopy height. With the reference p' at the treetops (panel 2 in Figure 10), the phase relationship of R_{pu} changes little because p' is vertically coherent (Figure 5), and the correlation R_{pu} mainly reflects the phase characteristics of the auto-correlation of u'.

Cross-correlation R_{up} with u' as the reference (panels 3 and 4 in Figure 10) illustrates that u' near the ground is vertically in-phase with p', and that the positive correlation is significant (0.6 to 0.7) inside the forest canopy. On the other hand, u' at treetop height poorly correlates with local p' but significant negative correlations (-0.4 to -0.3) and positive correlations (0.2 to 0.3) occur upwind and downwind, respectively. This agrees with observations (Shaw and Zhang, 1992; Zhuang and Amiro, 1994) that a region of overpressure appears near the intersection of the scalar microfront at the canopy top, upwind of the ejection of low momentum fluid, and downwind of the sweep of high momentum air from aloft.

Near the forest floor (panel 1 in Figure 11), the cross-correlation between the local time derivative of longitudinal velocity ($\partial u'/\partial t$) and the pressure gradient force in the streamwise direction ($-\partial p'/\partial x$) is greater than 0.8. However, there is no such correlation at the top of the forest (panel 2 in Figure 11). On the other hand, the correlation between $\partial u'/\partial t$ and the advective term $-u_j(\partial u'/\partial x_j)$ is about 0.2 near the surface (panel 3 in Figure 11) and approximately 0.9 at the top of the forest (panel 4 in Figure 11). These correlations indicate that an acceleration or deceleration in longitudinal velocity near the forest floor is caused primarily by a fluctuating pressure gradient force, while advection is minor but not negligible. They also provide more direct evidence to support the proposal of Shaw and Zhang (1992) that the pressure perturbations drive the fluctuations of longitudinal velocity near the forest floor. Moreover, the implication is that, on the average, near the forest floor, the total Lagrangian time derivative of the longitudinal velocity is dominated by the local (Eulerian) time derivative, i.e., the advective components are small, so that the streamwise pressure gradient force almost balances the local time derivative of the longitudinal velocity. In contrast, at the canopy top, the advective components of the velocity field dominate and the effect of fluctuating pressure gradient is negligible. Finally, in the middle of the forest, both advection
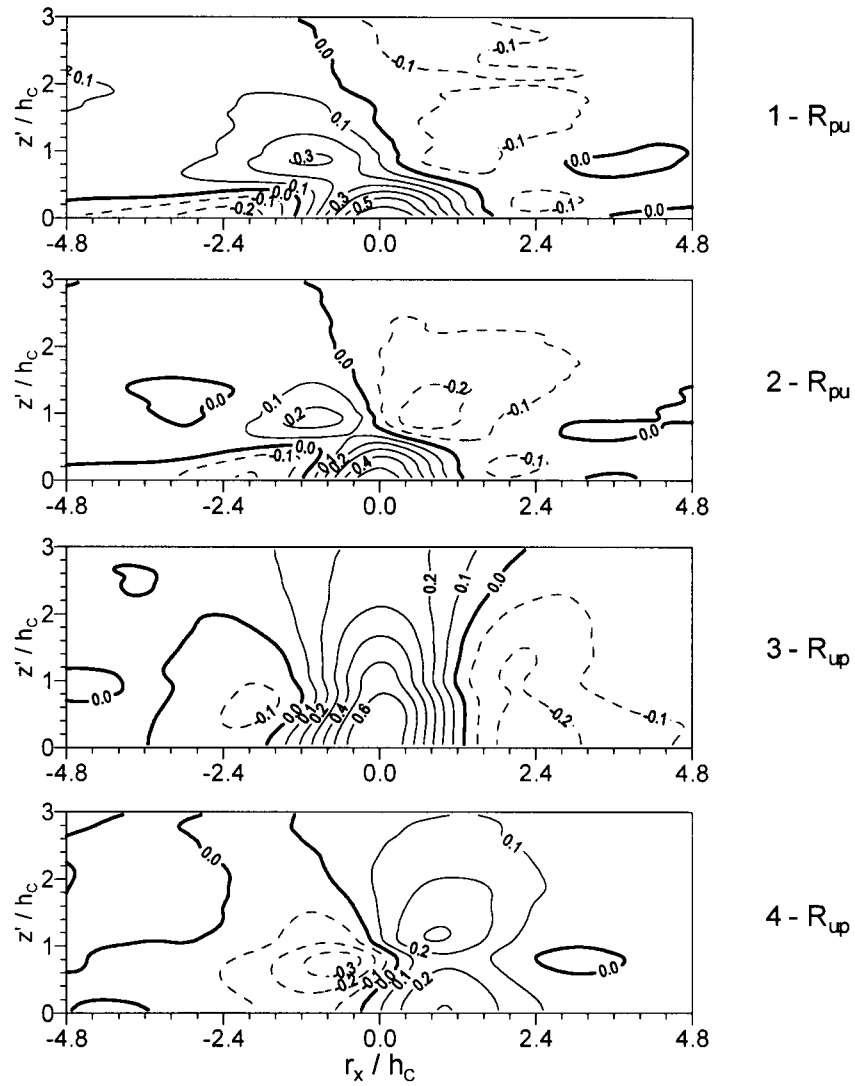
Figure 10. Zero-time-lag two-point cross-correlation between u' and p' with streamwise and vertical separations ($r_y = 0$). Panels 1 and 2 with $X_i = p'$; Panel 3 and 4 with $X_i = u'$; Panels 1 and 3 with X_i at $z = 0.05h_C$; Panel 2 and 4 with X_i at $z = 0.95h_C$.

and fluctuating pressure gradient are equally important in driving the longitudinal velocity, which is not shown for the sake of brevity.

The above results support the following paradigm for shear-driven turbulent flow within and above a forest canopy, expanded upon from Shaw and Zhang (1992). At the canopy top, the dominant advective components are associated with shear instability that creates large coherent structures (Gao et al., 1989; Raupach et al., 1989, 1991, 1996; Paw U et al., 1992). The strong shear during coherent
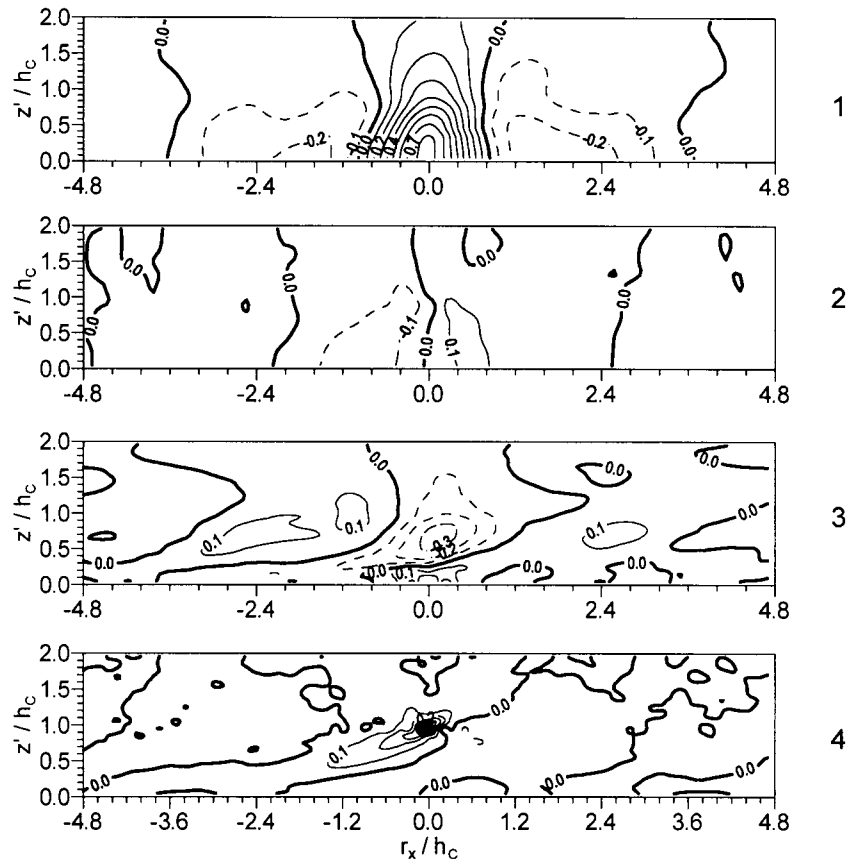
Figure 11. Zero-time-lag two-point cross-correlations between $\partial u'/\partial t$ and $-\partial p'/\partial x$ (panels 1 and 2) and between $\partial u'/\partial t$ and $-u_j(\partial u'/\partial x_j)$ (panels 3 and 4) with streamwise and vertical separations ($r_y = 0$). All with $X_i = \partial u'/\partial t$ which is at $z = 0.05h_C$ in panels 1 and 3 and at $z = 0.95h_C$ in panels 2 and 4.

motions (sweep/ejection events) is primarily responsible for the generation of the pressure pattern (Shaw et al., 1990; Shaw and Zhang, 1992; Zhuang and Amiro, 1994) that is vertically in-phase, causing a streamwise pressure gradient that drives the longitudinal velocity fluctuations (correlation >0.8) near the forest floor. To a lesser extent, but not negligible (correlation is about 0.2), are the advective components of longitudinal velocity fluctuations near the surface.

When averaging over time or over an extensive horizontal plane, the perturbations in the longitudinal velocity in the trunk space near the forest floor (driven by the pressure pattern associated with the sweep/ejection motion near treetop level) do not yield a net downward transfer of momentum. However, they do act as a source of the longitudinal component of turbulent kinetic energy in this region, as shown by Su et al. (1998b) from the horizontal average of $-u'(\partial p'/\partial x)$. Not
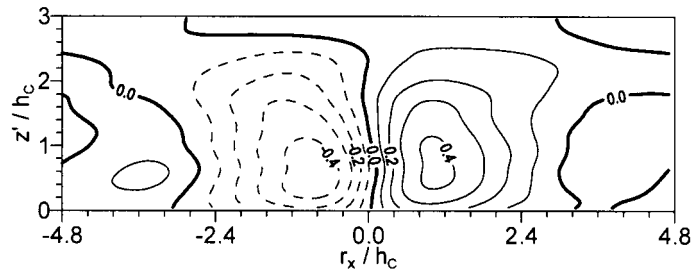
Figure 12. Zero-time-lag two-point cross-correlation between p' and w' with streamwise and vertical separations ($r_y = 0$), with $X_i = p'$ at $z = 0.05h_C$.

shown here for the sake of brevity is the calculation that u' in the trunk space is highly positively correlated with $-\partial p'/\partial x$. Because mean wind speed is relatively low in the trunk space, such a pressure-driven longitudinal velocity perturbation is likely to be of importance in studies of turbulent diffusion in this region.

Vertical velocity is essentially decorrelated from local pressure (Figure 12). Instead, the two quantities are negatively correlated when w' is displaced in the upwind direction, with peak correlation in the upper forest at $r_x/h_C = -0.8$, and positively correlated when w' is displaced in the downwind direction, with peak correlation approximately at the same height and $r_x/h_C = 1$. This phase relationship changes only slightly with height, as anticipated because both variables independently retain phase with separation in the vertical direction. These features are consistent with the relationship between vertical velocity and surface pressure illustrated by Shaw et al. (1990) such that peak pressure lies between the preceding ejection (updraft) and the following sweep (downdraft), with the same order of peak correlation (± 0.4). Shaw et al. (1990) found that positive and negative peak correlations appear at time lags of about ± 7 s and they estimated a translation velocity of 2.12 m s^{-1}, which yields a horizontal separation of about ± 0.8 of their forest height (18 m), and very close to our LES results (Figure 12).

3.2. CORRELATIONS IN THE y-z PLANE

3.2.1. *Auto-Correlations*
As expected from symmetry, auto-correlations of u', v' and s' with spatial displacements in a plane perpendicular to the streamwise direction exhibit no distinct tilt like their counterparts in the x-z plane (Figures 1–3). For the sake of brevity, we only show the auto-correlation of the longitudinal velocity (Figure 13), which shares some common features with wind-tunnel studies (Shaw et al., 1995). For example, with the reference level near the canopy top ($z/h_C = 0.95$), correlation contours show distinct negative side lobes for both negative and positive lateral separations that appear in the middle of the canopy and above. The magnitude of the negative correlation agrees with the wind-tunnel observation (peak correlation of about -0.15). The zero contours also appear at similar lateral separations (about
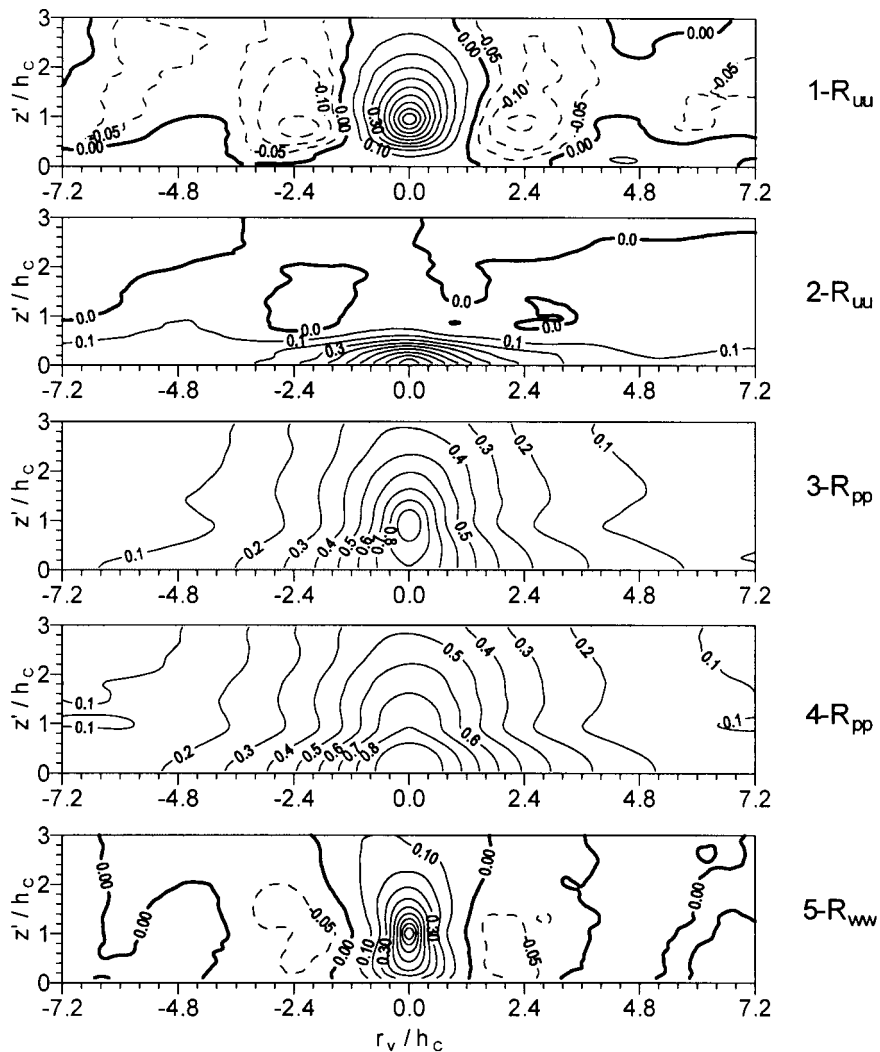
Figure 13. Zero-time-lag two-point auto-correlation with spanwise and vertical separations ($r_x = 0$) for u' (panels 1 and 2), p' (panels 3 and 4) and w' (bottom panel). The reference X_i is at the treetops in panels 1, 3 and 5, and at the first grid from the ground in panels 2 and 4. The interval for positive (solid) contours is 0.1 and that for negative (dashed) contours is 0.05.

$\pm 1.5h_C$), but the peak negative correlations from the LES are located approximately at $r_y/h_C = \pm 2.4h_C$, somewhat closer to the origin ($r_y/h_C = 0$) than the wind-tunnel observation (at $r_y/h_C = \pm 3h_C$) of Shaw et al. (1995).

However, for reference u' near the ground ($z/h_C = 0.05$), there is no significant negative correlation and the 0.3 contour extends laterally from $r_y/h_C = -2.4$ to $r_y/h_C = 2.4$, below $z'/h_C = 0.4$, indicating laterally in-phase characteristics of longitudinal velocity in the trunk space. In addition, the correlation decreases

to less than 0.1 above $z'/h_C = 0.5$ for all lateral separations, indicating that for zero streamwise separation, but with or without a lateral separation, longitudinal velocity in the trunk space is relatively isolated from that in the upper forest and immediately above. This is in contrast to the auto-correlations shown in Figure 1, which exhibit significant positive correlations between u' near the ground and that near the treetops when there is a streamwise separation between them.

The laterally in-phase feature of u' in the trunk space again indicates that longitudinal velocity perturbation in this region is largely associated with pressure perturbations that are also laterally in phase, as no negative correlations appear in the auto-correlations of p' (Figure 13), unlike equivalent correlations in the x-z plane (Figure 5). This indicates that the pair of positive and negative pressure perturbation regions associated with the coherent motions are not only vertically coherent (Figure 5), but also retain their phase in the spanwise direction (Figure 13). This provides a justification for the assumption employed by Zhuang and Amiro (1994) in simplifying the Poisson equation into a two-dimensional (x-z plane) integration to study pressure patterns during coherent motions.

Negative side lobes also appear in the auto-correlations of vertical velocity (Figure 13) with the same degree of correlation (-0.05) as the wind-tunnel observation (Shaw et al., 1995), and located at similar lateral separations (peak correlations at about $\pm 2h_C$). The auto-correlations of u' and w' with the reference near the treetops (Figure 13) suggest that at both sides of the sweep ($u' > 0$, $w' < 0$), there is a pair of ejection-like regions ($u' < 0$, $w' > 0$). This is further discussed below in relation to the cross-correlation between u' and w'.

3.2.2. *Cross-Correlations*

Longitudinal velocity at the top of the forest is negatively correlated with vertical velocity w' to a lateral separation of about $\pm 1.2h_C$ (Figure 14), and positive side lobes appear between $\pm 1.2h_C$ and $\pm 3.6h_C$ with slightly greater magnitudes (0.1 to 0.15) than the wind-tunnel measurement (0.05 to 0.1) by Shaw et al. (1995), while peak positive correlations are located at about the same lateral separation ($\pm 2h_C$). However, the positive side lobes disappear when u' near the ground is the reference, and the negative correlation is reduced to small values. This reduced correlation is not compensated by a lateral separation as it is by a streamwise separation (Figure 9). Again, this is because the acceleration in u' in the trunk space is largely driven by a fluctuating streamwise pressure-gradient force that is downstream of the downward motions (sweep), and the acceleration as a result of the gust penetrating through the forest is minor (the correlation between u' and nearby w' is on the order of -0.1).

The correlation with w' at treetop height as the reference (Figure 14) mainly reflects the characteristics of the auto-correlations of u' (Figure 13). Both the auto-correlations of u' and w' and the cross-correlation between them indicates that there is a pair of ejection-like regions in the middle of the forest and above at both sides of the sweep region. This is absent in the cross-correlations between u' and
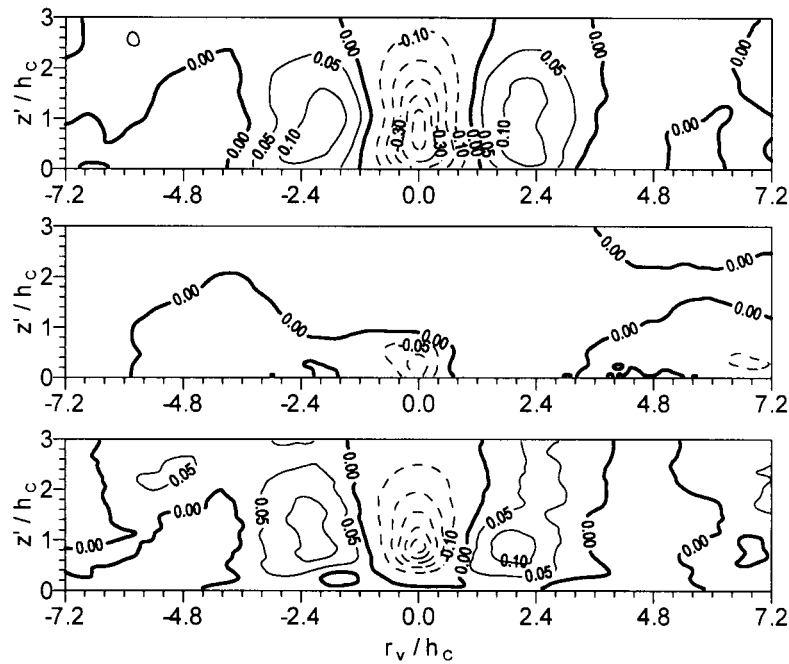
Figure 14. Zero-time-lag cross-correlation between u' and w' with spanwise and vertical separations ($r_x = 0$). Top panel: $X_i = u'$ at the treetops; Middle panel: $X_i = u'$ at the first grid from the ground; Bottom panel: $X_i = w'$ at the treetops is the reference. The interval for positive (solid) contours is 0.05 and that for negative (dashed) contours is 0.1 in the top and bottom panels, and the interval is 0.05 in the middle panel.

w' in the x-z plane when the reference is at the treetops (Figure 9). This is perhaps because, when the coherent motions move downwind, the positive correlation region between u' and w' in an x-z plane, regardless of which is the reference, is smeared out. On the other hand, the phase relationship between u' and w' in the lateral direction remains with little shift when the sweep/ejection is advected downstream.

Finally, both the auto-correlations (Figure 13) and the cross-correlations (Figure 14) in the y-z plane are approximately symmetric with the same positive and negative lateral separations from the origin $r_y / h_C = 0$. Such symmetry is not perfect, but is expected in theory as discussed in Shaw et al. (1995) where advantage was taken so that measurements were not duplicated at equal positive and negative lateral separations.

3.3. EULERIAN INTEGRAL TIME AND LENGTH SCALES

3.3.1. *Single-Point Integral Time Scale $T(z)$*

The single-point integral time scale $T(z)$ normalized by the mean wind speed at treetop level U_{hc} and the canopy height h_C for the longitudinal velocity is relatively constant inside the forest, with an average value on the order of 1 (Figure 15). A larger LES domain (run D) or a longer record of observation (30 minute) yielded a larger value of the integral time, and a greater rate of increase of $T(z)U_{hc}/h_C$ with height above the canopy, reaching a value of about 1.8 near twice the canopy height. The effect of finer grid resolution in LES or of a higher sampling frequency of observation is to reduce the integral time as a result of small-scale random turbulence smearing out the temporal coherence of larger-scale organized coherent motions. The agreement between LES run D and the 30-minute observation is reasonably good up to twice the canopy height.

For the scalar, $T(z)U_{hc}/h_C$ changes little above the forest, also with an average value on the order 1, but continuously increases with increasing depth into the forest. The effect of a larger LES domain or a longer time record of measurement is also a larger integral time scale, and a finer resolution in either space or time results in a smaller integral time. Excellent agreement between the LES run D and the 30-minute observation can be seen inside the forest, both showing that $T(z)U_{hc}/h_C$ increases from 1.3 at the treetops to about 2.2 at a third of the forest height. However, the LES yielded somewhat smaller values than the observation above $2h_C$.

For the vertical velocity, both the LES and the observation demonstrate that $T(z)U_{hc}/h_C$ changes little above the forest, with an average value on the order of 0.5, but increases with depth into the forest to about a third of the canopy height, below which observation is not available and the LES shows that it decreases again when approaching the forest floor. The relatively larger increase above $1.5h_C$ shown from LES runs A and C could be due to the limited vertical domain in the two runs. Above the canopy, the effect of LES domain size or measurement record length on the integral time for w' is similar to that for u' and s'. However, inside the forest, unlike the longitudinal velocity and the scalar, a larger LES domain or a longer record of observation yielded a somewhat smaller integral time for the vertical velocity. The effect of a finer resolution in space or time is the same as for the longitudinal velocity and scalar, to reduce the integral time scale, both within and above the forest.

Moreover, the integral time scales of u' and s' are more sensitive to the LES domain size or the measurement record than to the resolution in space or in time. In contrast, the integral time for w' is more sensitive to the spatial or temporal resolution than to the domain size or record length. For example, while our LES run D (largest domain) yielded better agreement with the 30-minute and 10 Hz observation on the integral time scales for u' and s', better agreement on the in-
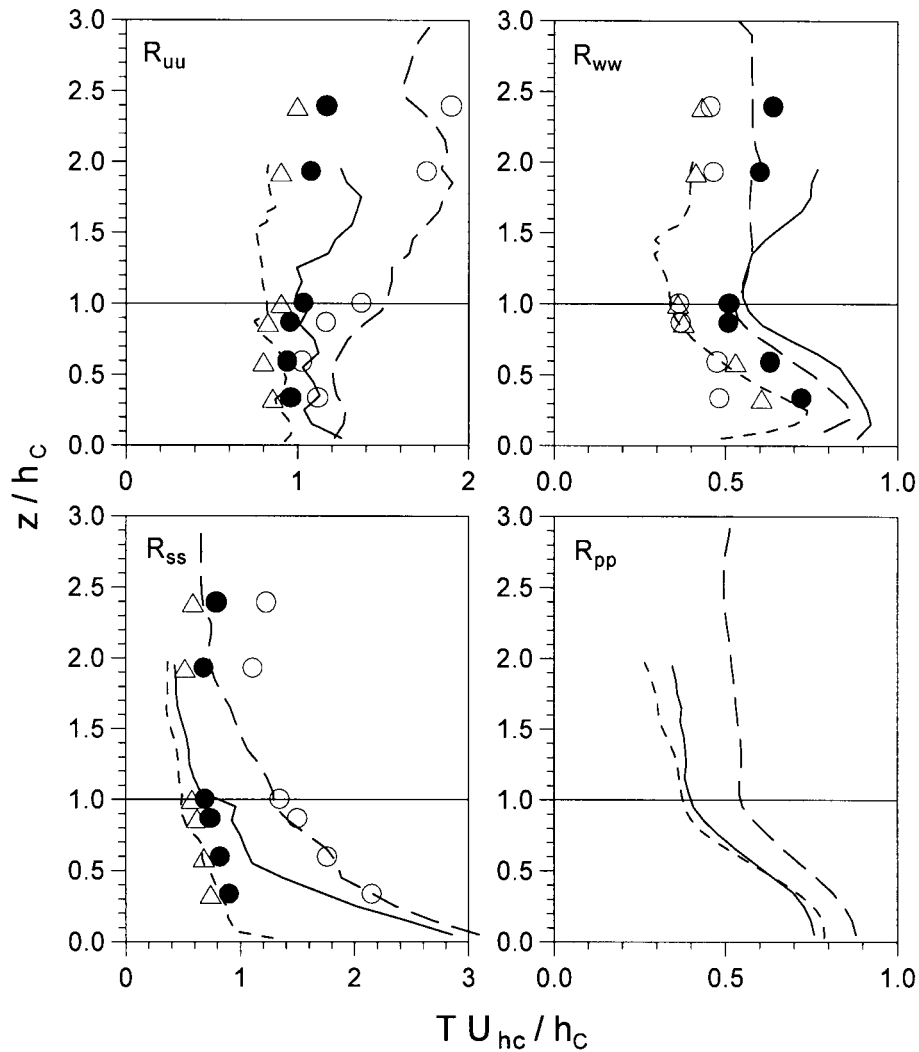
Figure 15. Single-point integral time scales normalized by the mean longitudinal velocity at the forest top U_{hc} and the height of the forest h_C. Solid curves: LES run A; Short-dashed curves: LES run C; Long-dashed curves: LES run D; Open circles: 30-minute 10 Hz observation; Open triangles: 5-minute 10 Hz observation; Closed circles: 5-minute 0.33 Hz observation.

tegral time for w' was obtained between LES run D and the 5-minute and 0.33 Hz observation.

Finally, not available from either field or wind-tunnel observations is the normalized single-point integral time scale for the static pressure perturbations shown from the LES work (Figure 15), which is approximately constant above the forest with a value on the order of 0.5 (LES run D), and increases with depth into the forest. A larger domain size (LES run D) yielded a greater normalized integral

time of p' than a smaller domain (LES run A) by about 0.1 inside the forest and less than 0.2 above the canopy. The impact of a finer grid resolution on the integral time scale of p' is less than that for the other variables because pressure is a spatial integral of the velocity field, and smaller-scale perturbations make a relatively smaller contribution to signal variance.

3.3.2. *Spatial Integral Streamwise Length Scale $L_x(z)$*

The effects of LES domain size and grid resolution on the magnitude of $L_x(z)$ are similar to those on the normalized single-point integral time scales. Thus, for simplicity, we only present the streamwise spatial integral length scale from the LES run D in Figure 16.

Inside the forest, $L_x(z)/h_C$ for the longitudinal velocity changes little with an average value of about 1.2. It increases slowly from 1.4 at the treetops to about 1.8 at 1.8 times the canopy height and decreases slightly above. This vertical pattern is similar to that in the wind-tunnel experiment but with smaller magnitudes. Shaw et al. (1995) showed that $L_x(z)/h_C$ was 2.2, 2.8, 3 and 2.9 at $z/h_C = 0.5$, 1, 2 and 4, respectively.

Similar to the normalized integral time scale for w' (Figure 15), $L_x(z)/h_C$ increases with depth into the forest to about a third of the canopy height and decreases again as the ground is approached. It also increases somewhat above twice the canopy height. Overall, $L_x(z)/h_C$ for the vertical velocity does not change much both within and above the forest, with an average of about 0.6, which is close to the value measured in the wind tunnel (Shaw et al., 1995). Above the forest, $L_x(z)/h_C$ for the scalar and static pressure are also quite constant, with average values of about 0.8 and 0.6, respectively. However, both increase with increasing depth into the forest.

A clear feature shown in Figure 16 is that the product of the single-point integral time scale $T(z)$ and the local mean longitudinal velocity $\bar{u}(z)$, is not a sensible approximation for the streamwise length scale $L_x(z)$. In particular, the former overestimates or underestimates the latter above or below treetop height, respectively. A comparison between the spatial integral streamwise length scales and the corresponding single-point integral time scales illustrates that they have very similar vertical patterns for the same variable. For example, both $L_x(z)$ and $T(z)$ for the scalar and the pressure increase with depth into the forest, while they change little above the canopy. This indicates that a single velocity may be appropriate to link $T(z)$ and $L_x(z)$. Using the mean longitudinal velocity at the treetops, we obtain a much better estimate of $L_x(z)$ than we do with the local mean longitudinal velocity (Figure 16).

3.3.3. *Spatial Integral Spanwise Length Scales $L_y(z)$*

Again, in general, a larger LES domain (run D) yields a greater value of $L_y(z)$ whereas a finer grid resolution somewhat reduces the magnitude of $L_y(z)$ (Figure 17). However, the vertical pattern of $L_y(z)$ for each variable essentially remains
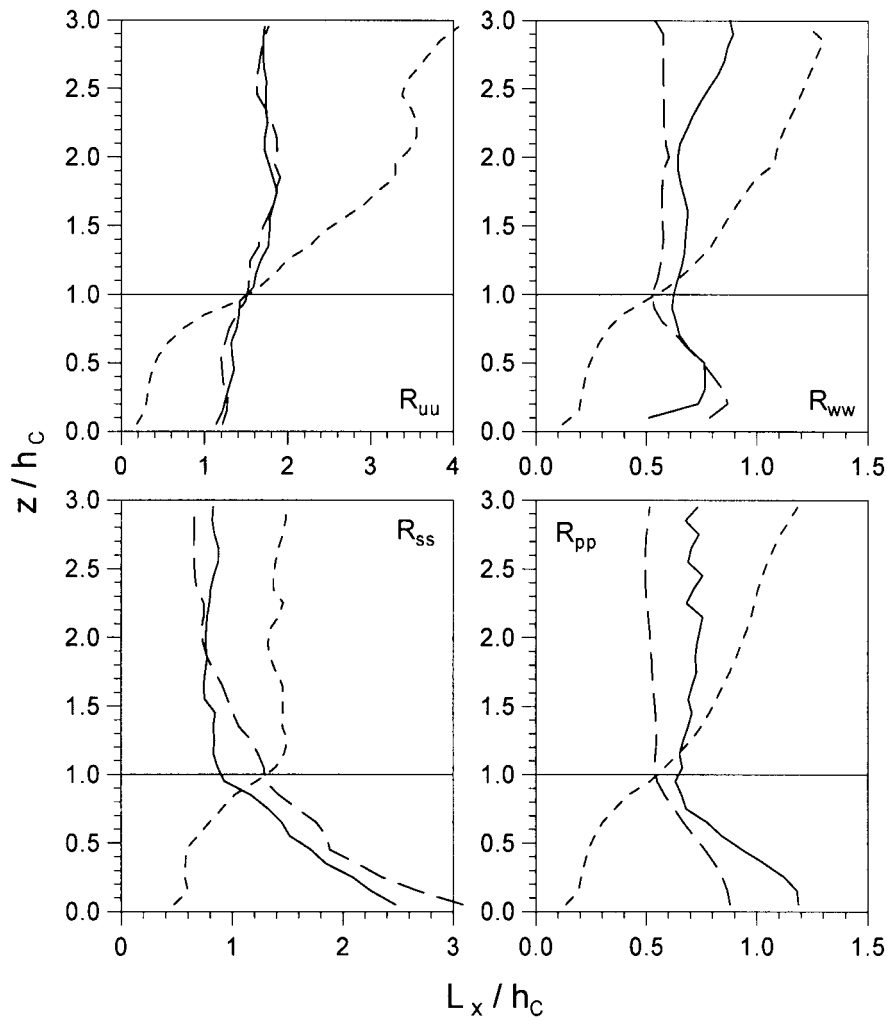
Figure 16. Streamwise length scales normalized by the height of the forest h_C from LES run D. Solid line: calculated from Equation (3); Short dashed curve: products of respective single-point integral time $T(z)$ and local mean longitudinal velocity $\bar{u}(z)$; Long dashed curve: products of single-point integral time $T(z)$ and the mean longitudinal velocity at the treetops.

unchanged. For example, $L_y(z)/h_C$ for the longitudinal velocity changes little in the upper forest and above the canopy, with an average value of about 0.5 (based on run D), but increases with depth into the forest. For the vertical velocity, there is a peak located between half and a third of the canopy height, while the length scale changes little above the canopy; only run D showed a slow increase from 0.4 at the treetops to about 0.5 at three times canopy height. The magnitudes of $L_y(z)/h_C$ for u' and w' in the upper forest and above the canopy generally agree with the
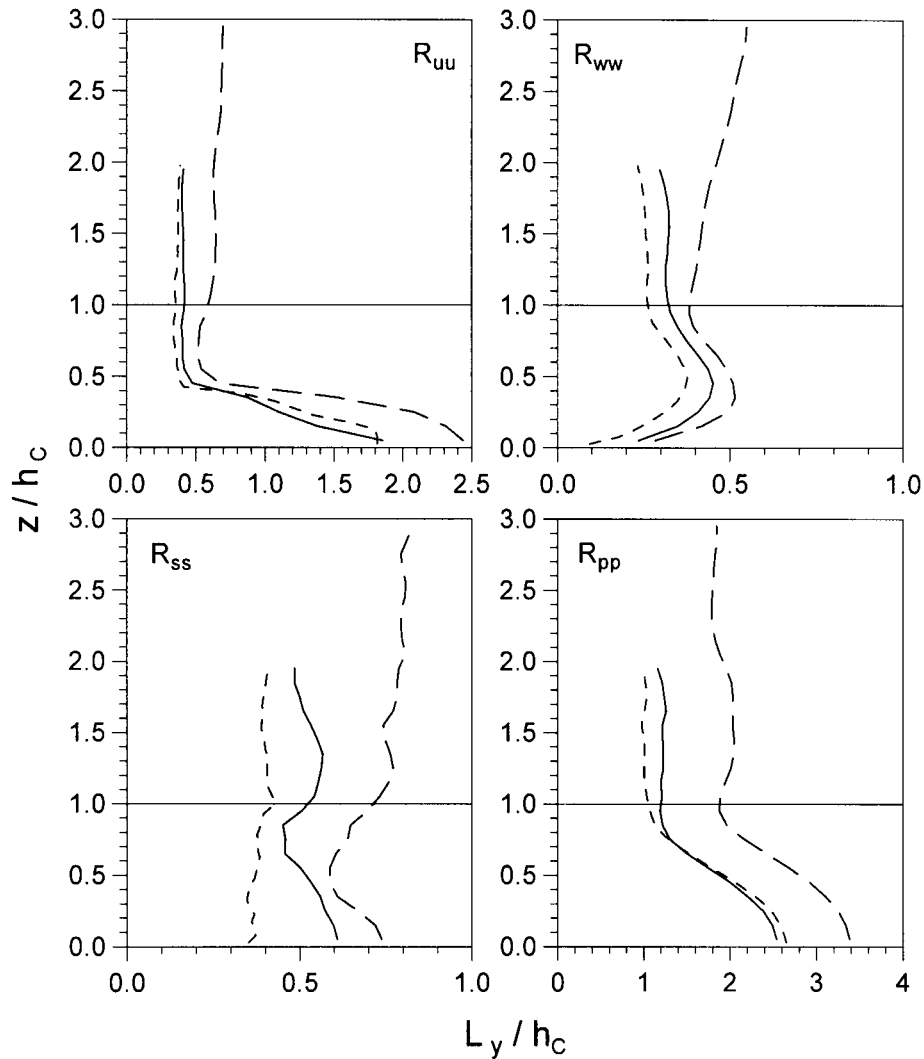
Figure 17. Spanwise integral length scales normalized by the forest height h_C. Solid curves: LES run A. Short dashed curves: LES run C. Long dashed curves: LES run D.

wind-tunnel measurements (Shaw et al., 1995) but no information in the lower half was available from their study.

For the scalar, $L_y(z)/h_C$ does not increase in the same fashion as $L_x(z)/h_C$ with increasing depth into the forest, and changes little both within and above the canopy with values between 0.6 and 0.8 (run D). For the static pressure, $L_y(z)/h_C$ also remains relatively constant above the forest, and increases with depth into the forest. At the same height, $L_y(z)$ is more than twice as large as $L_x(z)$, and also increases more quickly inside the canopy. It has been suggested that the pressure

field largely drives longitudinal velocity in the trunk space near the forest floor. Thus, it is natural, perhaps, that longitudinal velocity at this level follows the same pattern as static pressure in terms of its lateral length scale.

Both streamwise and spanwise spatial integral length scales presented above are likely to be smaller than the spatial scales of actual coherent structures in the longitudinal and lateral directions. This is because smaller-scale motions tend to destroy the spatial coherence of the larger-scale coherent motions, for example, finer grid resolution (run A) generally yielded smaller spatial integral length scales. In addition, because of the out-of-phase characteristics of u' and w' in the sweep and the ejection regions, some of the negative correlations such as those illustrated in Figure 13 perhaps should be included in calculating the integral length scales as discussed by Shaw et al. (1995), if the sweep and ejection ought to be considered as one physical entity.

3.4. CONVECTIVE VELOCITY

Although not shown here for the sake of brevity, lagged two-point auto-correlations with only streamwise separation exhibit elliptical shapes. A convective velocity (U_c) may be estimated from the slope of the major axis of the ellipses. In practice, for a given time lag τ, the streamwise separation $r_{x,\mathrm{max}}$ corresponding to the maximum correlation was found. Then, the slope is deduced from a linear regression of all the points ($r_{x,\mathrm{max}}$, τ). A second approach matches that of Shaw et al. (1995) such that the linear regression is performed over all the points (r_x, τ_{max}) where, for a given streamwise separation r_x, the time lag τ_{max} is found that maximizes the correlation.

Clear features in Figure 18 are that convective velocities calculated from lagged two-point correlations are larger than the local mean longitudinal velocity, and the second method yields somewhat larger values than the first approach. The values of U_c/U_{hc} in the middle of the forest (1.5 and 1.3) and at the treetops (1.7 and 1.5) deduced from the auto-correlations of u' and w', respectively, and estimated using the second method, agree with the wind-tunnel values very well. Both are in general agreement with many previous studies that larger-scale coherent motions are advected downwind at a speed higher than the local mean wind speed. For example, Gao et al. (1989) found a value of $U_c/U_{hc} = 1.14$ at the top of an 18-m tall deciduous forest by timing the passage of the sharp temperature microfronts observed at two towers separated by 25 m. Zhang et al. (1992) found a larger value of $U_c/U_{hc} = 1.6$ for a 6-m tall orchard canopy, also using temperature microfront transit time between two towers. Zhang et al. (1992) also determined that the translation speed from lagged correlation between the two towers agreed with that derived from the scalar microfront transit time. Three snapshots of a scalar microfront with time intervals of 30 seconds from LES run A are presented in Figure 19 to illustrate the downwind convection of a microfront. The average distance between streamwise locations of the same microfront at the canopy top is about $1.95h_C$, which yields
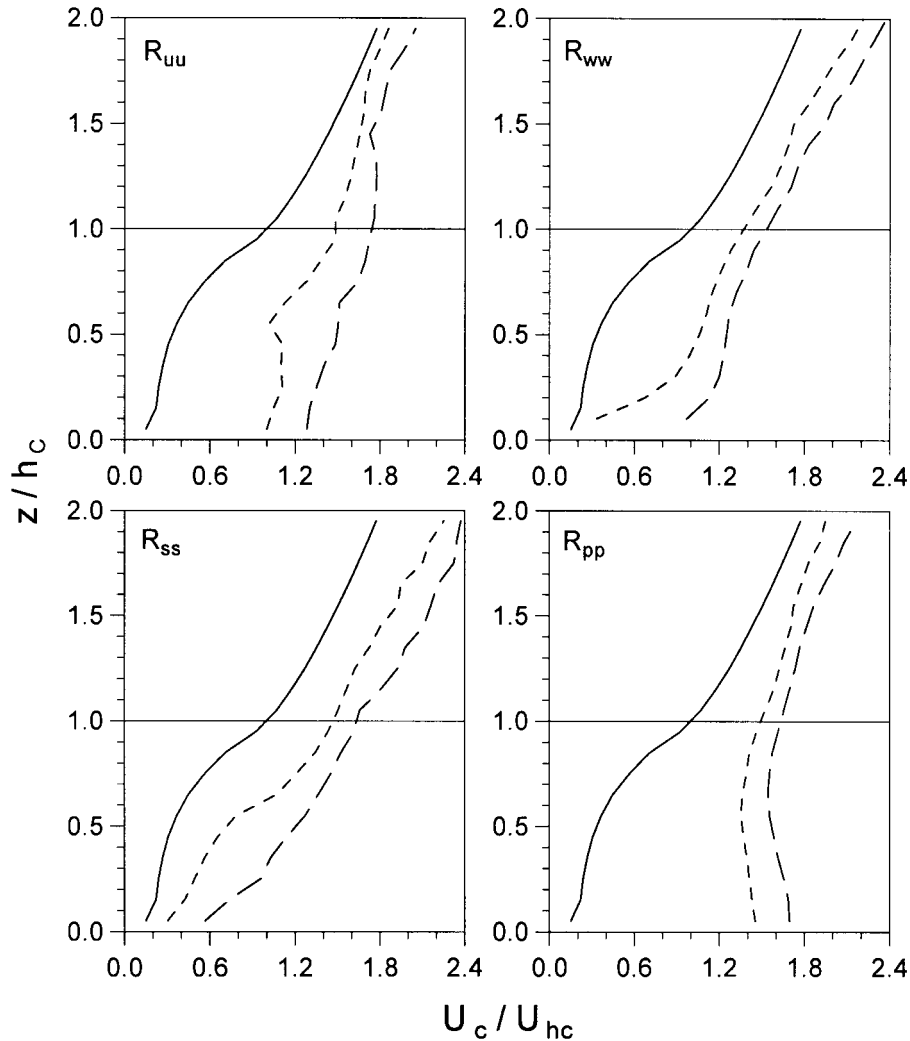
Figure 18. Vertical profiles of mean longitudinal velocity (solid curve) and convective velocities U_c calculated from lagged two-point auto-correlations from LES run D. Short dashed curve: based upon points $(r_{x,\max}, \tau)$. Long dashed curves: based upon points $(r_x, \tau_{\max})$. All velocities are normalized by the mean wind speed at the canopy height U_{hc}.

a normalized translation velocity U_c/U_{hc} of the microfront of about 1.37. This value is in general agreement with those (1.4 for u' and s', 1.3 for w' and 1.5 for p') estimated from the lagged auto-correlations at treetop height using the first approach. It is also noted that the average distance between the streamwise locations of the pressure peaks near the surface is also about $1.95h_C$ and, on average, the peak pressure is located just ahead (downstream) of corresponding microfront at the canopy top.
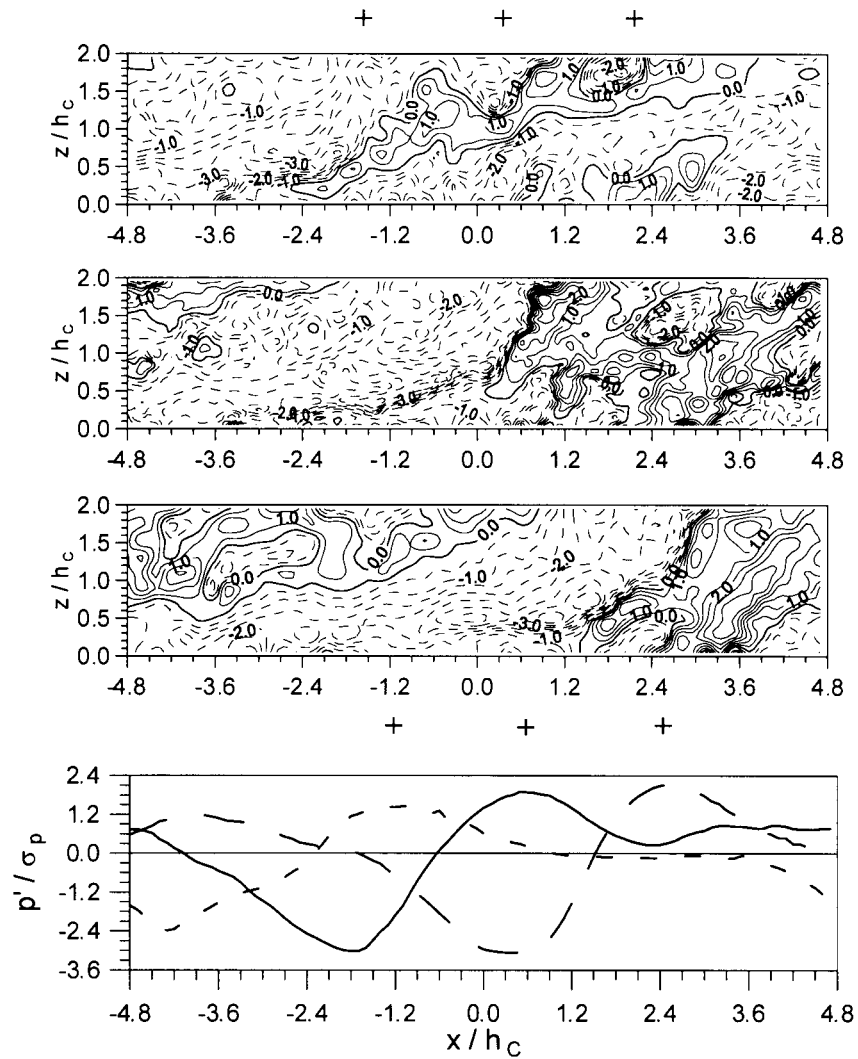
Figure 19. Three snapshots (30 seconds apart) of instantaneous fluctuating scalar concentration normalized by the characteristic scalar s_* from LES run A (top three panels). In the bottom panel are static pressure at the first grid, normalized by its standard deviation, corresponding to each snapshot of the scalar microfront. The plus symbols indicate the approximate streamwise locations of the scalar microfronts near the canopy top or of the peak static pressure near the surface.

It should be noted that the convective velocities calculated from the lagged two-point correlations may not represent the velocity at which a coherent structure is carried downstream as an entity. This is because all scales of turbulent motions contribute to the two-point correlations, and the convective velocity itself is likely scale-dependent (Comte-Bellot and Corrsin, 1971). One would expect a coherent structure to have an approximately constant translation velocity, otherwise

the structure would not maintain its integrity over time. For example, Zhang et al. (1992) found the convective velocity of the temperature features to be nearly constant with height above and within a 6-m tall orchard canopy. The scalar microfront shown in Figure 19 from the LES run A maintains its entity with no significant deformation when it is convected downstream at a velocity that appears approximately constant with height. This indicates that the convective velocities calculated from lagged two-point correlations, which increase with height above the canopy in both current LES analysis and the wind-tunnel study (Shaw et al., 1995), are not entirely representative of the translation velocity of the coherent structures, reflecting influences of turbulent motions with scales different from the coherent structures. In addition, Zhang et al. (1992) found that translation velocities estimated by timing temperature microfronts passing two towers along the mean wind direction agreed well with those using lagged-two-point correlations, both of which were nearly independent of height between the heights of $0.27h_C$ and $1.5h_C$. This may be because they first bandpass filtered (0.5 to 0.005 Hz) their raw 10 Hz data so that signals outside this range contributed little to the correlations. Both field observation Gao et al. (1989) and the LES (Su, 1996) illustrate that the time series of turbulent signals inside the forest do not have as much high frequency fluctuation as those above the canopy. This may explain why convective velocity estimated from lagged two-point correlation changes more slowly with height inside the canopy than above. In addition, the observation that convective velocity calculated from static pressure perturbations increases less quickly with height than those from u', w' and s' is perhaps because pressure at a single point is influenced by the velocity everywhere in the domain and thus random small-scale fluctuations have less influence.

4. Conclusions

Two-point correlation fields calculated from the resolved-scale output of large-eddy simulations of atmospheric flow through and above a forest show many of the same distinctive characteristics seen in analyses of data from a real forest, an orchard, and from a wind tunnel. However, large-eddy simulation creates much more extensive spatial detail of the flow field than is otherwise available, and also includes the perturbation pressure field.

Principal features of the analyses include downwind tilts in the auto-correlations of longitudinal and lateral velocities and of the scalar, while vertical velocity and pressure are vertically coherent. An important aspect of the streamwise velocity auto-correlation relates to the correlation near the forest floor. Streamwise velocity at treetop height positively correlates with longitudinal velocity in regions of the relatively open trunk space in both upstream and downstream directions. The former can also be found in the scalar and spanwise velocity auto-correlations, and may be interpreted as a signature of downwind advection of a sloping coherent

structure (microfront), whereas the latter has no equivalent in the case of the lateral velocity and the scalar, yet was not unexpected since a similar feature has been reported from temporal correlations in a real forest. Cross-correlations between velocity and static pressure support an earlier proposal that flow near the forest floor is mainly driven by a pressure field created by the strong wind shear aloft, although some evidence of non-negligible advective effects was also demonstrated. The cross-correlation between the local time derivative of longitudinal velocity and the pressure gradient also shows evidence that advection is a dominant process at the canopy top, when compared to the local pressure gradient.

Comparisons of lagged two-point correlations with vertical separation between field observations in a real forest and the present simulation exhibit remarkable agreement in terms of both the phase relationship (normalized time lags for peak correlations) and the magnitude of correlations. Many of the features of such lagged correlations match those of equivalent zero-time-lag spatial correlations determined from the LES flow fields. This implies that many of the spatial aspects of the flow field and of a scalar distribution may be correctly inferred from a measured time series at a single tower. To a large extent, this is a result of the observation that major flow and scalar patterns move downstream at a speed that is rather independent of height through the canopy.

At the canopy height, convective velocities calculated from lagged two-point correlations using the LES output agree with the translation velocity estimated from instantaneous snapshots of a scalar microfront, and are also consistent with previous estimates in the wind tunnel using the same approach. While studies in an orchard exhibited a nearly height-independent translation velocity (using lagged correlations, where measurement records were pre-conditioned to filter out the effects of unwanted small scales), the present LES analysis yields lagged two-point correlation convective velocities that increase with height above the forest. This implies an influence of small-scale motions, which were not removed prior to analysis. Estimates of convective velocity are considerably greater than the local mean longitudinal velocity, with the greatest difference being inside the canopy. Likewise, a single velocity (the mean longitudinal velocity at the forest top) is found to be more appropriate than the local mean velocity to link single-point integral time scales to the corresponding streamwise Eulerian length scales directly integrated from zero-time-lag two-point correlations.

Finally, effects of domain size and grid resolution in the LES on the two-point correlations are discussed in conjunction with the effects of the record length and sampling frequency of measurements in the field. Major phase characteristics in the two-point correlation fields essentially remained the same between the four LES runs with various domain sizes and grid resolutions. However, a more extensive domain (LES run D) did yield improvement in the agreement on the magnitude of correlations with field observations, especially above the canopy. Although the horizontal domain of LES run D was more than 19 times the canopy height and is considered to be adequate based upon the spatial scales of the scalar microfronts

observed in the field, there is evidence that the greatest vertical domain of six times canopy height in our LES runs is still somewhat limited, especially for correlations above twice the canopy height. A finer grid resolution mainly results in a faster rate of decrease of correlations. This is not unexpected because smaller-scale motions tend to be more random and degrade the spatial coherence associated with larger and more organized coherent motions. Likewise, proper filtering of a rapidly sampled turbulent record could be important in order for the two-point correlation to be more representative of the coherent motions.

Acknowledgements

References

Bergström, H. and Högström, U.: 1989, 'Turbulent Exchanges above a Pine Forest II. Organized Structures', *Boundary-Layer Meteorol.* **49**, 231–263.

Berkooz, G., Holmes, P., and Lumley, J. L.: 1993, 'The Proper Orthogonal Decomposition in the Analysis of Turbulent Flows', *Ann. Rev. Fluid Mech.* **25**, 539–575.

Bessem, J. M. and Stevens, L. J.: 1984, 'Cross-Correlation Measurements in a Turbulent Boundary Layer above a Rough Wall', *Phys. Fluids* **27**, 2365–2366.

Brown, G. L. and Thomas, A. S. W.: 1977, 'Large Structure in a Turbulent Boundary Layer', *Phys. Fluids* **20**, 243–252.

Brunet, Y., Finnigan, J. J., and Raupach, M. R.: 1994, 'A Wind Tunnel Study of Air Flow in Waving Wheat: Single-Point Velocity Statistics', *Boundary-Layer Meteorol.* **70**, 95–132.

Comte-Bellot, G. and Corrsin, S.: 1971, 'Simple Eulerian Time Correlation of Full- and Narrow-Band Velocity Signals in Grid-Generated, "Isotropic" Turbulence', *J. Fluid Mech.* **48**, 273–337.

Conklin, P. S. and Knoerr, K. R.: 1994, 'The Role of Static Pressure Fluctuations in the Structure of Turbulence within and above a Hardwood Forest Canopy', in preprint, *The American Meteorological Society 21st Conference on Agricultural and Forest Meteorology*, San Diego, CA, pp. 175–178.

Gao, W., Shaw, R. H., and Paw U, K. T.: 1989, 'Observation of Organized Structure in Turbulent Flow within and above a Forest Canopy', *Boundary-Layer Meteorol.* **47**, 349–377.

Moin, P. and Moser, R. D.: 1989, 'Characteristic-Eddy Decomposition of Turbulence in a Channel', *J. Fluid Mech.* **200**, 471–509.

Newmann, H. H., den Hartog, G., and Shaw, R. H.: 1989, 'Leaf Area Measurements Based on Hemispheric Photographs and Leaf-Litter Collection in a Deciduous Forest during Autumn Leaf-Fall', *Agric. For. Meteorol.* **45**, 325–345.

Paw U, K. T., Brunet, Y., Collineau, S., Shaw, R. H., Maitani, T., Qiu, J., and Hipps, L.: 1992, 'On Coherent Structures in Turbulence above and within Agricultural Plant Canopies', *Agric. For. Meteorol.* **61**, 55–68.

Raupach, M. R., Coppin, P. A., and Legg, B. J.: 1986, 'Experiments on Scalar Dispersion within a Plant Canopy, Part I: The Turbulent Structure', *Boundary-Layer Meteorol.* **35**, 21–52.

Raupach, M. R.: 1989, 'Applying Lagrangian Fluid Mechanics to Infer Scalar Source Distributions from Concentration Profiles in Plant Canopies', *Agric. For. Meteorol.* **47**, 85–108.

Raupach, M. R., Finnigan, J. J., and Brunet, Y.: 1989, 'Coherent Eddies in Vegetation Canopies', in *Proceedings 4th Australian Conference on Heat and Mass Transfer*, Christchurch, New Zealand, pp. 75–90.

Raupach, M. R., Antonia, R. A., and Rajagopalan, S.: 1991, 'Rough-Wall Turbulent Boundary Layers', *Appl. Mech. Rev.* **44**, 1–25.

Raupach, M. R., Finnigan, J. J., and Brunet, Y.: 1996, 'Coherent Eddies and Turbulence in Vegetation Canopies: The Mixing-Layer Analogy', *Boundary-Layer Meteorol.* **78**, 351–382.

Shaw, R. H., Den Hartog, G., and Neumann, H. H.: 1988, 'Influence of Foliar Density and Thermal Stability on Profiles of Reynolds Stress and Turbulence Intensity in a Deciduous Forest', *Boundary-Layer Meteorol.* **45**, 391–409.

Shaw, R. H., Paw U, K. T., Zhang, X. J., Gao, W., den Hartog, G., and Neumann, H. H.: 1990, 'Retrieval of Turbulent Pressure Fluctuations at the Ground Surface beneath a Forest', *Boundary-Layer Meteorol.* **50**, 319–338.

Shaw, R. H. and Zhang, X. J.: 1992, 'Evidence of Pressure-Forced Turbulent Flow in a Forest', *Boundary-Layer Meteorol.* **58**, 273–288.

Shaw, R. H., Brunet, Y., Finnigan, J. J., and Raupach, M. R.: 1995, 'A Wind Tunnel Study of Air Flow in Waving Wheat: Two-Point Velocity Statistics', *Boundary-Layer Meteorol.* **76**, 349–376.

Su, H.-B.: 1996, *Numerical Simulations of Plant-Atmosphere Interactions Using Large-Eddy Simulation and Coupled Leaf and Canopy Models*, Ph.D. Thesis, University of California, Davis, CA, 239 pp.

Su, H.-B., Shaw, R. H., Paw U, K. T., Moeng, C.-H., and Sullivan, P. P.: 1998a, 'Turbulent Statistics of Neutrally Stratified Flow within and above a Sparse Forest from Large-Eddy Simulation and Field Observations', *Boundary-Layer Meteorol.* **88**, 363–397.

Su, H.-B., Paw U, K. T., Shaw, R. H., and Moeng, C.-H.: 1998b, 'Large-Eddy Simulation of Pressure-Gradient-Velocity Covariance and Its Parameterization within and above a Forest', in preprint, *The American Meteorological Society 23rd Conference on Agricultural and Forest Meteorology*, Albuquerque, NM, pp. 229–232.

Wilczak, J. M. and Businger, J. A.: 1984, 'Large-Scale Eddies in the Unstably Stratified Atmospheric Surface layer. Part II: Turbulent Pressure Fluctuations and the Budgets of Heat Flux, Stress and Turbulent Kinetic Energy', *J. Atmos. Sci.* **41**, 3551–3567.

Wilson, D. K.: 1996, 'Empirical Orthogonal Function Analysis of the Weakly Convective Atmospheric Boundary Layer. Part I: Eddy Structures', *J. Atmos. Sci.* **53**, 801–823.

Wilson, D. K. and Wyngaard, J. C.: 1996, 'Empirical Orthogonal Function Analysis of the Weakly Convective Atmospheric Boundary Layer. Part II: Eddy Energetics', *J. Atmos. Sci.* **53**, 824–841.

Zhang, C., Shaw, R. H., and Paw U, K. T.: 1992, 'Spatial Characteristics of Turbulent Coherent Structures within and above an Orchard Canopy', in S. E. Schwartz and W. G. N. Slim (co-ordinators), *Precipitation Scavenging and Atmosphere-Surface Exchange*, Vol. 2, Hemisphere Publishing Co., Washington, DC, pp. 741–751.

Zhuang, Y. and Amiro, B. D.: 1994, 'Pressure Fluctuations during Coherent Motions and their Effects on the Budgets of Turbulent Kinetic Energy and Momentum Flux within a Forest Canopy'. *J. Appl. Meteorol.* **33**, 704–711.

Zhuang, Y.: 1996, 'A Lower-Order Model of Coherent Structures in the Convective Atmospheric Surface Layer', *Quart. J. Roy. Meteorol. Soc.* **122**, 1075–1094.